JAN 23 1952

NACA

RESEARCH MEMORANDUM

THE USE OF AREA SUCTION FOR THE PURPOSE OF DELAYING SEPARATION

OF AIR FLOW AT THE LEADING EDGE OF A 63° SWEPT-BACK WING -

EFFECTS OF CONTROLLING THE CHORDWISE DISTRIBUTION

OF SUCTION-AIR VELOCITIES

By Woodrow L. Cook and Mark W. Kelly

Ames Aeronautical Laboratory
Moffett Field, Calif.

CLASSIFIED DOCUMENT

This material contains information affecting the National Defense of the United States within the meaning of the espionage laws, Title 18, U.S.C., Secs. 793 and 794, the transmission or revelation of which in any manner to an unauthorized person is prohibited by law.

NATIONAL ADVISORY COMMITTEE
FOR AERONAUTICS
WASHINGTON
January 14, 1952

NATIONAL ADVISORY COMMITTEE FOR AERONAUTICS

RESEARCH MEMORANDUM

THE USE OF AREA SUCTION FOR THE PURPOSE OF DELAYING SEPARATION

OF AIR FLOW AT THE LEADING EDGE OF A 63° SWEPT-BACK WING -

EFFECTS OF CONTROLLING THE CHORDWISE DISTRIBUTION

OF SUCTION-AIR VELOCITIES

By Woodrow L. Cook and Mark W. Kelly

SUMMARY

An investigation was conducted to determine the effectiveness of area suction when used to prevent air-flow separation at the leading edge of a 63° swept-back wing. Initial results of this investigation have been reported previously in NACA RM A50H09, 1950. The present report presents the results of tests made with the chordwise distribution of the suction-air velocities controlled to give lower total-flow quantity requirements. The main part of the investigation dealt with the delay effected in air-flow separation and the improvements made on the aerodynamic characteristics of the wing with area suction designed for a lift coefficient of 0.77. Changes in lift, drag, and pitching moment were correlated with pressure distribution and flow studies.

The effectiveness of area suction with the suction-air velocities controlled to be equal at all chordwise points was verified by the improvements made in the aerodynamic characteristics of the wing. With a flow coefficient of 0.0034, large improvements were made in drag and pitching-moment characteristics from a lift coefficient of 0.25 to a lift coefficient of about 0.80. The flow coefficients required in this investigation for a given increment of lift with no air-flow separation were about 0.4 of those required in the previous investigation. The minimum values of flow coefficient required were about 10 times the theoretical value. The chordwise extents of area suction required at the outboard section were in good agreement with the estimated values. However, it was found that the values of chordwise extent estimated at the inboard sections were considerably larger than required in the investigation. This was believed to be due to the natural spanwise boundary-layer flow existing on the three-dimensional wing.

INTRODUCTION

A previous investigation (reference 1) has shown that area suction was effective in delaying the occurrence of air-flow separation at the leading edge of a 63° swept-back wing. The results of that investigation indicated that the chordwise and spanwise extents of area suction required to prevent separation for a given lift coefficient were in good agreement with the values estimated by the method derived in reference 1. However, the quantity of flow required to prevent separation was much greater than the value predicted by the two-dimensional theory of reference 2.

Since the most desirable feature of area suction as a method of boundary-layer control at high lift coefficients is the extremely low flow quantity requirements indicated by theory, an analysis was made to determine possible reasons for the large difference (approximately 25 times) between the theoretical and experimental values of flow coefficient. One reason, suggested in reference 1, was evident upon determination of the chordwise distribution of suction-air velocities. It was found that, due to having a porous surface of constant porosity at all chordwise points, the value of the suction-air velocity increased continually from a minimum value near the leading edge to a maximum value at the rearmost chordwise edge of the porous area. This condition did not satisfy the assumption made in reference 2 where the suction-air velocities were assumed to be constant at all chordwise points. From the analysis, it was concluded that the flow coefficient could be reduced by approximately 60 percent or to about 10 times the theoretical value if the chordwise distribution of suction-air velocities were controlled to be constant, as assumed in the theory.

The investigation was continued on the 63° swept-back wing in an effort to reduce the flow quantity requirements without jeopardizing the effectiveness of area suction in preventing leading-edge air-flow separation. In an effort to compensate for the external pressure variation so as to obtain equal suction-air velocities at all chordwise points, the thickness of the porous material at a given section was varied from a minimum thickness at the leading edge to a maximum thickness at the rearmost point of the porous opening. The thickness variation of the porous material was designed for a wing lift coefficient of 0.77 at a Reynolds number of 5.2 × 10⁶. For this thickness variation, the suction-air velocities were assumed to be 10 times the theoretical value, since at the leading edge the suction-air velocities required in the previous investigation were approximately 10 times the value estimated by theory. The pressure distributions for unseparated flow at a design wing lift coefficient of 0.77 were obtained by extrapolating the pressure distributions attained with area suction in the

investigation of reference 1. In addition to the tests concerned with reducing of flow quantity requirements, brief studies were made of (1) the chordwise extent of porous area for lower design lift coefficients (to further verify the reasoning used in reference 1 for estimating the extent of porous area), (2) the possibility of using the natural boundary-layer drain of the highly swept wing to reduce the amount of boundary-layer air to be removed by suction, and (3) the effect of boundary-layer control when used with a deflected trailing-edge flap.

The investigation was conducted in the Ames 40- by 80-foot wind tunnel. The results of the tests are presented in this report.

NOTATION

The data are presented in the form of standard NACA coefficients and symbols which are defined as follows:

b   wing span, feet

c   chord, measured parallel to the plane of symmetry, feet

c_n chord, measured normal to the leading edge, feet

$\bar{c}$ mean aerodynamic chord $\left(\dfrac{\int_0^{b/2} c^2 dy}{\int_0^{b/2} c\, dy} \right)$, feet

c_l section lift coefficient $\left(\dfrac{1}{c} \int_0^c P dx \cos \alpha - \dfrac{1}{c} \int_0^t P dz \sin \alpha \right)$

C_D drag coefficient $\left(\dfrac{drag}{q_0 S} \right)$

C_L lift coefficient $\left(\dfrac{lift}{q_0 S} \right)$

C_m pitching-moment coefficient computed about the quarter-chord

point of the mean aerodynamic chord $\left(\dfrac{\text{pitching moment}}{q_o S \bar{c}}\right)$

C_Q flow coefficient $\left(\dfrac{Q}{U_o S}\right)$

l length of porous material, measured along surface normal to leading edge, inches

p_o free-stream static pressure, pounds per square foot

p_l local static pressure, pounds per square foot

P airfoil pressure coefficient $\left(\dfrac{p_l - p_o}{q_o}\right)$

q_o free-stream dynamic pressure, pounds per square foot

Q volume of air removed through porous surface, cubic feet per second based on standard density

R Reynolds number $\left(\dfrac{U_o \bar{c}}{\nu}\right)$

S wing area, square feet

t airfoil thickness, feet, or thickness of porous material, inches

u local velocity parallel to surface and inside boundary layer, feet per second

U local velocity parallel to surface at outer edge of boundary layer, feet per second

U_{max} maximum local velocity, feet per second

U_o free-stream air velocity, feet per second

w_o suction-air velocity normal to surface, feet per second

x   chordwise coordinate parallel to plane of symmetry, feet

y   spanwise coordinate perpendicular to plane of symmetry, feet

z   ordinate of airfoil surface normal to chordline and boundary-
         layer coordinate normal to the surface, feet

α angle of attack, degrees

Δp pressure drop across porous material, pounds per square foot

ν kinematic coefficient of viscosity, square feet per second

MODEL AND APPARATUS

The details of the model and its installation are shown in fig-
ures 1, 2, and 3. The same wing was used in the investigation presented
in reference 1. The fuselage had a maximum diameter of 3.68 feet which
is about 0.91 of the diameter of the fuselage used in the investigation
of reference 1.

The inboard 60-percent span of the wing was equipped with a
trailing-edge split flap. The flaps were 20 percent of the chord
normal to the leading edge and were deflected downward 45° measured
in a plane normal to the hinge line.

The leading-edge portion of the wing was constructed of continuous
metal-mesh sheet extending from 5 percent of the streamwise chord on
the lower surface of the wing to 20 percent of the streamwise chord on
the upper surface. The mesh sheet, the same as that described in
reference 1, was 0.01 inch thick, had 1600 holes per square inch, and
had 19-percent open area. The surface was not covered with aircraft
linen as in the previous investigation. Instead, the surface was
backed with a porous, white wool, hard felt material which was held
firmly in place against the mesh surface by a screen of large mesh
supported by leaf springs. The wool felt had a weight of approximately
4 pounds per square yard for material of 1/2-inch thickness. The
porous material varied in thickness chordwise, as shown in figure 4,
from a minimum thickness (1/32 inch) at the leading edge to a maximum
thickness at the aft edge of the porous opening. The variations of
thickness were dependent on the external surface pressure variation at
the particular spanwise section. Theoretically, the thickness varia-
tion would be constantly changing spanwise as well as chordwise due to
the spanwise load change. For easier construction and installation,
the spanwise change was accomplished in six steps as shown in figure 4.

The change from one section to the next was not large and the thickness
at any point was not more than 15 percent from the theoretically cor-
rect value at the point. A compromise on the thickness variation was
necessary at the outboard 15 percent of the span as the construction
of the leading edge would not allow as large a variation of thickness
as shown in figure 4. Therefore, a linear variation of wool felt
thickness was used, as shown in the figure.

Calibration tests were made of the flow resistance characteristics
of the porous material. The wool felt and the metal mesh were tested
together, with no flow tangential to the surface. The calibration
curves for different thicknesses of the porous material are shown in
figure 5. The curves are linear in the lower range of velocities.
The pressure differential required to induce a given suction-air veloc-
ity shows a nearly linear variation with the thickness of the material.
Some inconsistency in samples of the same thickness was noted as shown
for two samples of 1/8-inch-thick wool felt by curves (a) and (b),
figure 5. All other check calibrations of felts of the same thickness
showed better agreement.

The suction system was the same as described in reference 1. How-
ever, more accurate control of the spanwise variation of duct pressures
to meet the requirements of the spanwise load change was attained with
a new valve system. The flow coefficient, duct pressures, and wing-
surface pressures were measured in the same manner as in the investiga-
tion of reference 1. Table I shows the location of rows of pressure
orifices on the upper and lower surface parallel to the plane of
symmetry.

TESTS

Force and pressure-distribution measurements and some tuft studies
were made on the basic wing and the wing with suction through an angle-
of-attack range at zero sideslip. The data were obtained at a Reynolds
number of 5.2×10^6 based on a mean aerodynamic chord of 8.64 feet.
The basic-wing tests were obtained with the porous surface sealed by
covering with a nonporous cellulose tape.

The tests with suction were made with area suction applied to
the entire span of the wing. The porous surface thickness distribution
used in all the tests was designed for optimum performance at a wing lift
coefficient of 0.77.

The chordwise extents of area suction required for various lift
coefficients were calculated by the method discussed in reference 1.
For the determination of these extents the chordwise velocity

distributions presented for moderate angles of attack in reference 1 were extrapolated to higher lift coefficients. Figure 6 shows calculated chordwise extents required for several stations along the span as a function of lift coefficient.

For the investigation of the wing designed for a lift coefficient of 0.77, the chordwise extent of area suction varied from 1.4 percent of the streamwise chord at 30-percent span to 6.2 percent of the streamwise chord at 90-percent span (configuration A). The values for this configuration are tabulated for five spanwise sections in figure 3. Tests were also made with chordwise extent of area suction required for wing lift coefficients of 0.68 and 0.59 (configurations B and C). A test was made with the chordwise extent of area suction of configuration C reduced over the inboard stations (configuration D). The distribution of chordwise extent of area suction for the three configurations B, C, and D are also shown in the table in figure 3. A test was made with configuration A and a partial-span, trailing-edge split flap.

CORRECTIONS

Standard tunnel-wall corrections for a straight wing of the same area and span as the swept-back wing have been applied to angle-of-attack and drag-coefficient data. This procedure was followed since a brief approximate analysis indicated that tunnel-wall corrections were approximately the same for straight and swept wings of the size under consideration. The following increments were added:

$$\Delta\alpha = 0.48 \ c_L$$

$$\Delta c_D = 0.0084 \ c_L^2$$

The corrections for interference of the struts were not known; however, these corrections were believed not to be of sufficient magnitude to significantly affect the results. All flow coefficients were corrected to standard sea-level temperature conditions. The thrust of the exhaust air was measured at an angle of attack of 0°. It was found that the thrust was not of large enough magnitude to effect the drag results.

RESULTS AND DISCUSSION

Basic Wing

The lift, drag, and pitching-moment characteristics (fig. 7) are essentially the same as the results shown in reference 1 for the basic wing with a fuselage of slightly larger diameter. The severe increases in the rate of drag rise, the large movements of the aerodynamic center indicated by the pitching moment, and the causes of these changes are discussed in detail in reference 1.

Wing Designed for a Lift Coefficient of 0.77 and a Flow Coefficient of 0.0030

Force data.- The lift, drag, and pitching-moment characteristics for the basic wing and for configuration A, designed for a lift coefficient of 0.77 at a flow coefficient of 0.0030 (about 10 times theory), are shown in figure 8. The large increases in the rate of drag rise and large movements of the aerodynamic center indicated by the pitching moment were delayed from a lift coefficient of 0.25 for the basic wing to a lift coefficient of about 0.80 for configuration A. A total flow coefficient of 0.0034 was required at a lift coefficient of 0.77 (α=17.4°). The duct pressure coefficients at the four spanwise sections for this flow coefficient were as follows:

Spanwise station	0.45b/2	0.60b/2	0.75b/2	0.90b/2
Duct pressure coefficient	-20.0	-23.0	-27.5	-27.0

At slightly lower flow coefficients and duct pressures, the increased rate of drag rise and large movements of the aerodynamic center occurred at lift coefficients less than 0.80.

The drag coefficient, at a lift coefficient of 0.80 with area suction applied at a flow coefficient of 0.0034, is approximately 60 percent less than the drag coefficient of the basic wing. The pitching-moment variation indicates a gradual forward movement of the aerodynamic center starting at about a wing lift coefficient of 0.55 which is followed by a large movement forward above a lift coefficient of approximately 0.80.

Pressure data and flow studies.- The cause of variations in drag and pitching moment shown by the force data for this wing can be

deduced from the changes shown by the pressure distributions and ·tuft
studies. The relatively small changes in the longitudinal character-
istics that occur between a lift coefficient of 0.55 and 0.80 are
believed to be due to separation of air flow from the trailing edge,
whereas the abrupt, large changes occurring at lift coefficients above
0.80 are the result of air-flow separation at the leading edge. The
section pressure distributions (fig. 9) indicate that above an angle
of attack of 12.3° (C_L = 0.55) the changes that occurred in the pres-
sure distributions at the outboard sections are typical of the changes
associated with trailing-edge separation; the variation of pressure
coefficient with angle of attack for several chordwise points at the
90-percent spanwise section (fig. 10) emphasizes these changes. The
pressure coefficients near the trailing edge show a sudden decrease in
pressure above an angle of attack of 12.3°. At the same angle of
attack an increase in pressure occurs in the vicinity of the midchord.
The flow studies (fig. 11) show an area of rough flow which starts at
the outboard trailing edge of the wing and increases in size until at
an angle of attack of 17.4° (C_L = 0.77) the area has spread forward at
the tip to nearly the leading edge and inboard at the trailing edge to
at least the 60-percent spanwise station. Above an angle of attack of
12.3°, the lift curve of the section at the 90-percent span station
(fig. 12) tends toward the rounded lift curve typical of section lift
curves where trailing-edge separation is occurring. There is no evi-
dence of air-flow separation at the leading edge (fig. 9) up to an
angle of attack of 17.4° (C_L = 0.77). The pressure coefficients near
the leading edge (fig. 13) show steady increases negatively, with
increasing lift coefficient, and the tufts show smooth flow except in
the area discussed previously where trailing-edge separation prevails.
Above a lift coefficient of 0.77, the air flow separated near the lead-
ing edge as indicated by the sharp decrease in pressure coefficients
and by the tuft action. The occurrence of this form of separation
defines the maximum section lift coefficient at each of the sections
(e.g., fig. 12, 90-percent spanwise section $c_{l\,max}$ = 0.88 at an angle
of attack of 17.4°).

    It is of interest to note that although leading-edge separation ·
occurred near the design lift coefficient at the outboard sections, the
separation did not progress to the inboard sections until much higher
lift coefficients. This would seem to indicate that the flow of the
boundary-layer air toward the tip of the highly swept wing acted as a
natural boundary-layer control for· the inboard sections, thus allowing
the sections to go to higher lift coefficients than anticipated. It
was therefore considered likely that the chordwise extent of suction
could be less than that indicated by two-dimensional theory at all
sections inboard of the critical outboard area.

Flow quantity requirements.- The flow coefficient required to obtain a lift coefficient of 0.77 with no leading-edge separation was 0.0034. Tests were made with considerably higher flow coefficients than 0.0034, but the pressure distributions and the tuft studies indicated no effect on the initial occurrence of air-flow separation at the outboard sections. The chordwise extent of suction at these sections was thus indicated to be correct for the design conditions. It is possible that the forward progression of the boundary of the separated air-flow area from the trailing edge may be a factor limiting the maximum section lift rather than the chordwise extent of suction. From the tuft-study observation, however, it appeared that this limit would be at a somewhat higher lift coefficient than 0.77. The value of 0.0034 is somewhat greater than 10 times the theoretical value of 0.00030 shown in figure 14[1] for a wing lift coefficient of 0.77. Some of the difference in the values of the flow coefficient required experimentally and the value of 10 times theory that was anticipated can probably be attributed to the variation of the porous material thickness at the outboard 15 percent of the span. However, it is apparent that a major part of the reduction in flow coefficient from approximately 25 times theory to 10 times theory, which was the aim of this investigation, was realized. In both the present and the previous phase of the investigation, the minimum effective suction-air velocities near the leading edge have been about 10 times the values determined by the theory of Thwaites, as applied in reference 1. It is believed the following facts account for some of the discrepancy between theoretical and experimental flow quantities. The theory assumes a continuously porous material of ideal smoothness, whereas the porosity of the material used in the study was achieved by means of closely spaced holes and the surface was not ideally smooth. The magnitude of the distance between the holes, the hole size, and the roughness were of the order of the boundary-layer thickness and it is quite likely that each factor contributed significantly to increasing the required suction-air velocities.

In considering further means of reducing the flow quantities required, an examination has been made of the limitations imposed by maintaining equal suction-air velocities at all chordwise points.

---

[1] It should be noted that the theoretical flow-coefficient curve was determined using the method of Thwaites (reference 2) but with the use of the extrapolated chordwise velocity distributions of reference 1. This gave higher values of flow coefficient than determined in reference 1 where theoretically calculated pressure distributions were used to determine the flow coefficient.

A different and seemingly logical condition would be to have the
suction-air velocities vary as a function of the adverse chordwise
pressure gradient. The suction-air velocities would then vary from
the required value near the leading edge, which would be a maximum,
to a minimum value at the aft edge of the porous opening. Tests of
this variation of suction-air velocities were not possible due to the
construction of the leading-edge portions of the wing. A method of
determining this possible optimum chordwise distribution of suction-
air velocities is discussed in the appendix and is based on the theory
of Schlichting (reference 3).

Wing With Chordwise Extent of Area Suction
for Lift Coefficients of 0.68 and 0.59

Tests were made with the chordwise extent of area suction for
design wing lift coefficients of 0.68 and 0.59 (configurations B and C)
as well as for the design wing lift coefficient of 0.77 (configura-
tion A) discussed previously. The same variation of porous material
thickness was used in these tests as was used for a design wing lift
coefficient of 0.77. Therefore, the flow coefficients can only be
qualitatively compared with theoretical values since for each lift
coefficient the theoretical chordwise variation of porous material
thickness should be somewhat different.

For the several configurations, figure 15 indicates that no large
changes in the rate of drag rise or in the movement of the aerodynamic
center occurred before the design lift coefficients were reached. The
large variations in drag and pitching moment were caused by the separa-
tion of the air flow at the leading edge, as was the case for the
design lift coefficient of 0.77 discussed previously.

Flow quantity requirements.- The flow coefficient used for each
configuration was the minimum value that could be employed with no
occurrence of leading-edge air-flow separation up to the design lift
coefficient. Large increases in the flow coefficient in each case had
no effect on the initial occurrence of separation at the critical out-
board sections. Therefore, for the three design lift coefficients,
the initial occurrence of separation was controlled by the chordwise
extent of area suction at the outboard sections provided that sufficient
suction-air velocities were available. The flow coefficients required
for the three design lift coefficients are compared in the following
table to 10 times the theoretical value shown in figure 14:

Design lift coefficient	Flow coefficient 10 times theory	Flow coefficient required experimentally
C_L = 0.59, Config. C	0.0015	0.0016
C_L = .68, Config. B	.0022	.0026
C_L = .77, Config. A	.0030	.0034

Figure 16 shows the variation with angle of attack of the leading-edge pressures at the 90-percent spanwise section for the optimum configuration discussed in reference 1 and for the three configurations discussed in this report. For the case of reference 1, the decrease in the rate of pressure rise indicating separation occurred at angle of attack of about 9° with a flow coefficient of 0.0029; whereas with configuration C of this investigation and a much lower flow coefficient, 0.0016, the decrease did not occur until an angle of attack of approximately 13°. For the other two configurations (B and A of this investigation), the decrease in the rate of pressure rise occurred at angle of attack of about 15° and 17°, respectively.

Wing With Chordwise Extent of Area Suction
Reduced at the Inboard Sections

As noted previously, experiment indicated that the chordwise extent of area suction was larger than necessary at the sections inboard of the critical area near the tip. The extent of area suction at the inboard sections was reduced to approximately 50 percent of the value determined theoretically for a wing lift coefficient of 0.59 (configuration D, fig. 3). The aerodynamic characteristics of this configuration are compared to those of configuration C in figure 17. The effects of leading-edge separation in either case are not evident until a lift coefficient of 0.59 (α = 13.3°). Separation then progresses spanwise more rapidly in the case of configuration D. This is shown by the variation of pressure coefficient near the leading edge with angle of attack (fig. 18) for the two configurations tested.

The flow coefficient required with the reduced chordwise extents of area suction at the inboard section was 0.0013, which is less than the value of 0.0016 required with the extent of porous surface for configuration C.

Wing With Area Suction Used in Conjunction
With Deflected Trailing-Edge Flaps

A brief investigation was made in an effort to find the effective-
ness of area suction when used in conjunction with a 60-percent-span
trailing-edge split flap. The chordwise extent of area suction was
the same as for a design lift coefficient of 0.77 (configuration A).
The aerodynamic characteristics are shown in figure 19 for the wing
with the flap deflected both with and without area suction. For a
flow coefficient of 0.0033 which was the maximum that could be used,
the drag, pitching moment, and the pressure distributions show that
the effects of leading-edge air-flow separation were delayed from about
a lift coefficient of 0.40 to a lift coefficient of 0.80.

The section lift curves and the pressure distributions indicate
that there was a considerable carry-over of loading to the unflapped
portion of the wing. Although the end of the flap was at 60-percent
span, there was an increment of section lift carry-over of about 0.15
at 90-percent span as may be seen in figure 20. The leading-edge
pressure coefficients (fig. 21) at the 90-percent spanwise section
show that separation occurred at the leading edge at an angle of attack
of about 18° with no flap deflection and at an angle of attack of about
14° with the flap deflected. The minimum pressure in each case is
nearly equal. The initial occurrence of separation on the wing with
the flap deflected was in the same area as without the flap deflected.

CONCLUSIONS

The following conclusions were derived from the results of the
wind-tunnel investigation of area suction with controlled suction-air
velocities applied in the region of the leading edge of the 63° swept-
back wing:

1. Area suction was effective in delaying the occurrence of
leading-edge air-flow separation from a lift coefficient of 0.25 to a
design lift coefficient of 0.77.

2. The improvements made in the drag and pitching-moment charac-
teristics were affected with considerably lower values of flow coeffi-
cient with uniform suction-air velocities than with uniform porosity.

3. The chordwise extents of area suction required at the outboard
sections of the wing were in good agreement with the predicted values.
However, at the sections inboard of the critical outboard area, con-
siderably less extent of suction was required than was predicted.

4. Area suction was effective in controlling leading-edge separation when used with a partial-span trailing-edge split flap.

Ames Aeronautical Laboratory
    National Advisory Committee for Aeronautics
        Moffett Field, Calif.

APPENDIX

ADDITIONAL CONSIDERATIONS ON THE

CHORDWISE DISTRIBUTION OF SUCTION

The porous leading edge of the model tested in this investigation was designed to give constant suction-air velocities at all chordwise points at a given spanwise station. It was found that separation could be delayed on the 63° swept-back wing with lower flow requirements than for the surface of constant porosity used in the investigation of reference 1. The question arises as to whether additional reduction in the flow requirements might be made by further reduction in the suction-air velocities along the aft portions of the porous leading edge. From physical considerations such a distribution of suction-air velocity should still be capable of preventing separation since the adverse pressure gradients which the boundary layer must overcome are highest near the leading edge.

In reference 3, Schlichting outlines an approximate theoretical method for the calculation of the growth of the laminar boundary layer on two-dimensional profiles with arbitrary distributions of suction-air velocity. Schlichting's method is essentially an extension of the Kármán-Polhausen method for an impermeable surface to include the effects of suction or blowing through a porous surface. The method is based on the momentum equation for the laminar boundary layer on a porous surface.

$$U^2 \frac{d\theta}{dx} + (2\theta + \delta^*) U \frac{dU}{dx} - U w_0 = \nu \left(\frac{\partial u}{\partial y}\right)_0 \tag{1}$$

and assumed boundary-layer velocity profiles of the form (equation 10, reference 3)

$$\frac{u}{U} = 1 - e^{-\eta} + K \left(1 - e^{-\eta} - \sin \frac{\pi}{6} \eta\right), \quad 0 \le \eta \le 3$$

$$\frac{u}{U} = 1 - (K+1) e^{-\eta}, \quad \eta \ge 3 \tag{2}$$

where

$\eta = \frac{y}{\delta_1}$ measure of the nondimensional boundary-layer thickness

K form parameter of the velocity profiles

The quantity K is a function of both the pressure distribution and
the suction-air velocity. This family of velocity profiles when used
with the momentum equation results in the first-order, nonlinear dif-
ferential equation (equation 30, reference 3)

$$\frac{dZ^*}{dx^*} = \frac{G(k,k_1)}{U/U_0} \tag{3}$$

where

$$Z^* = \left(\frac{\theta}{c}\right)^2 R$$

$x^* = \frac{s}{c}$ nondimensional arc length along the airfoil surface

δ^* displacement thickness $\left[\int_0^\infty \left(1 - \frac{u}{U}\right)dy\right]$,feet

θ momentum thickness $\left[\int_0^\infty \frac{u}{U}\left(1 - \frac{u}{U}\right)dy\right]$,feet

$$k = Z^* \frac{d(U/U_0)}{dx^*}$$

$$k_1 = -\frac{w_0}{U_0}\sqrt{R\,Z^*}$$

The function $G(k,k_1)$ is rather complicated. However, it has been
plotted and tabulated in figure 6 and table 3 of reference 3 so that
the integration of equation 3 by the isocline method (reference 4) is
not difficult.

In reference 3, an example is calculated to obtain the growth of
the laminar boundary layer over an airfoil with uniform suction applied.
The problem of more practical interest, however, is somewhat different
from these examples in that the suction applied at the porous surface
is the unknown, and it is desired to calculate the distribution of
suction-air velocity that is just sufficient to keep the boundary layer
from separating. This problem can be solved by the same method with
the following considerations. The value of k at separation is equal

to -0.0721. Schlichting suggests that $k = -0.0682$ be used as an index of separation because computational difficulties are encountered as the value of $k = -0.0721$ is approached. The value of Z_s^* representing imminent separation can be calculated from

$$Z_s^* = \frac{-0.0682}{d(U/U_o)/dx^*} \qquad (4)$$

since, for any given profile, the velocity gradient $\dfrac{d(U/U_o)}{dx^*}$ is known as a function of x^*. The curve $Z_s^* = f(x^*)$ is plotted on the isocline plot and represents a boundary which the curve $Z^* = f(x^*)$ for the boundary layer may approach but not cross if separation is to be avoided. The computation is begun at the stagnation point and is performed in the conventional manner for the region of favorable gradient where no suction is needed, as shown in reference 3. As the curve $Z^* = f(x^*)$ approaches the region of adverse velocity gradients the slope of the curve, dZ^*/dx^*, is chosen so that the separation boundary is avoided. Then $G(k,k_1)$ can be obtained from equation 3. Then, since k is known, the value of the suction parameter k_1 can be obtained from the plot of $G(k,k_1)$ against k and k_1 (fig. 6 of reference 3). This procedure is continued to the chordwise station where no suction is needed. When the isocline computation is completed, values of Z^* and k_1 will be known at a series of points on the airfoil; from these the corresponding suction-air velocities can be calculated from

$$\frac{w_o}{U_o} = \frac{-k_1}{\sqrt{R \, Z^*}}$$

The method just outlined is limited to two-dimensional flows, but may be applied to a swept wing by the use of the principles of the simple sweep theory as used in reference 1. This approach was used to estimate the chordwise distribution of suction-air velocity necessary to avoid separation at the 90-percent span station of the 63° swept-back wing at a wing lift coefficient of 0.77. The resulting suction-air velocity distribution is shown in figure 22. The results indicate that the suction-air velocities required near the leading edge are much higher than those a short distance aft. (The horizontal line at $w_o/U_o = 0.012$ is the suction-air velocity calculated by the method of reference 2 and is included for comparison. At the leading edge the suction-air velocity calculated by Schlichting's method is approximately three times this value.) The calculations were stopped at $x/c = 0.06$ since it was known from the results of the test that no suction was needed aft of this point.

In employing the method of reference 3 to calculate the suction-air-velocity distribution, it was found that suction was necessary ahead of the minimum pressure point. (See fig. 22.) The highest suction-air velocities for which this theory is valid are limited to values of w_0/U_0 which are of the order of magnitude of δ/c. These velocities are considerably less than those used in the present investigation wherein unseparated flow was maintained without suction applied ahead of the leading edge.

Figure 23 presents a comparison at the 90-percent span station of three possible chordwise suction-air velocity distributions having the same critical suction-air velocity at the leading edge. The upper curve represents the distribution that would have been obtained from the wing of reference 1 if it had been taken to a lift coefficient of 0.77. The horizontal line at $w_0/U_0 = 0.12$ is approximately the experimental suction-air velocity distribution for the model used in this report. The lowest curve is that of figure 22 multiplied by a factor so that the suction-air velocity at the leading edge corresponds to that required experimentally. Assuming that these curves are typical of the suction-air velocity requirements on the rest of the wing span, it appears that, by reducing the suction-air velocities aft of the leading edge, a considerable saving in flow coefficient and power requirements should be obtained.

REFERENCES

1. Cook, Woodrow L., Griffin, Roy N. Jr., and McCormack, Gerald M.:
    The Use of Area Suction for the Purpose of Delaying Separation
    of Air Flow at the Leading Edge of a 63° Swept-Back Wing.
    NACA RM A50H09, 1950.

2. Thwaites, B.: A Theoretical Discussion of High-Lift Aerofoils
    With Leading-Edge Porous Suction. R.&M. No. 2242, British A.R.C.,
    1946.

3. Schlichting, H.: An Approximate Method for Calculation of the
    Laminar Boundary Layer with Suction for Bodies of Arbitrary
    Shape. NACA TM 1216, 1949.

4. Kármán, Theodore von, and Biot, M. A.: Mathematical Methods in
    Engineering. McGraw-Hill Book Co., Inc., New York and London,
    1st ed., 1940, pp. 6 to 8.

CONFIDENTIAL

TABLE I. - LOCATION OF PRESSURE ORIFICES

Spanwise position of orifices measured perpendicular to plane of symmetry	
Station number	Percent semi-span
1	30
2	45
3	60
4	75
5	90

Chordwise positions of orifices on upper and lower surfaces at each station, measured in per-cent of the streamwise chord	
Orifice number	Percent chord
1	0
2	.25
3	.50
4	1.0
5[a]	1.5
6[b]	2.5
7[c]	3.5
8[d]	5.0
9[e]	7.5
10[f]	10.0
11[g]	15.0
12	20.0
13	30.0
14	40.0
15	50.0
16	60.0
17[h]	70.0
18	80.0
19	90.0
20[i]	95.0
21[j]	97.5

[a]On station 1, orifice 5 on the upper surface, inoperative
[b]On station 1, orifice 6 on the upper surface, inoperative
[c]On station 2, orifice 7 on the upper surface, inoperative
[d]On stations 1 and 5, orifice 8 on upper surface, inoperative; on all stations, orifice 8 on the lower surface was omitted
[e]On stations 4 and 5, orifice 9 on upper surface inoperative
[f]On station 1, orifice 10 on upper surface, inoperative; on station 3, upper surface orifice 10 was located at 12-percent chord
[g]On station 1, orifice 11 on upper surface, inoperative
[h]On station 3, orifice 17 on upper surface, inoperative
[i]On station 4, orifice 20 on lower surface, inoperative
[j]On station 5, orifice 21 on lower surface, inoperative

NACA

CONFIDENTIAL

Wing	
Sweep	63°
Aspect ratio	3.5
Taper ratio	0.25
Twist	0°
Dihedral	0°
Incidence	0°
Airfoil section	NACA 64A006
Area	208.3 sq ft
Fuselage	
Fineness ratio	11.4
Radius at	
station x	$1.840\left(1-\left(\frac{x}{23}-1\right)^2\right)^{3/4}$ ft

All dimensions in feet
unless otherwise noted.
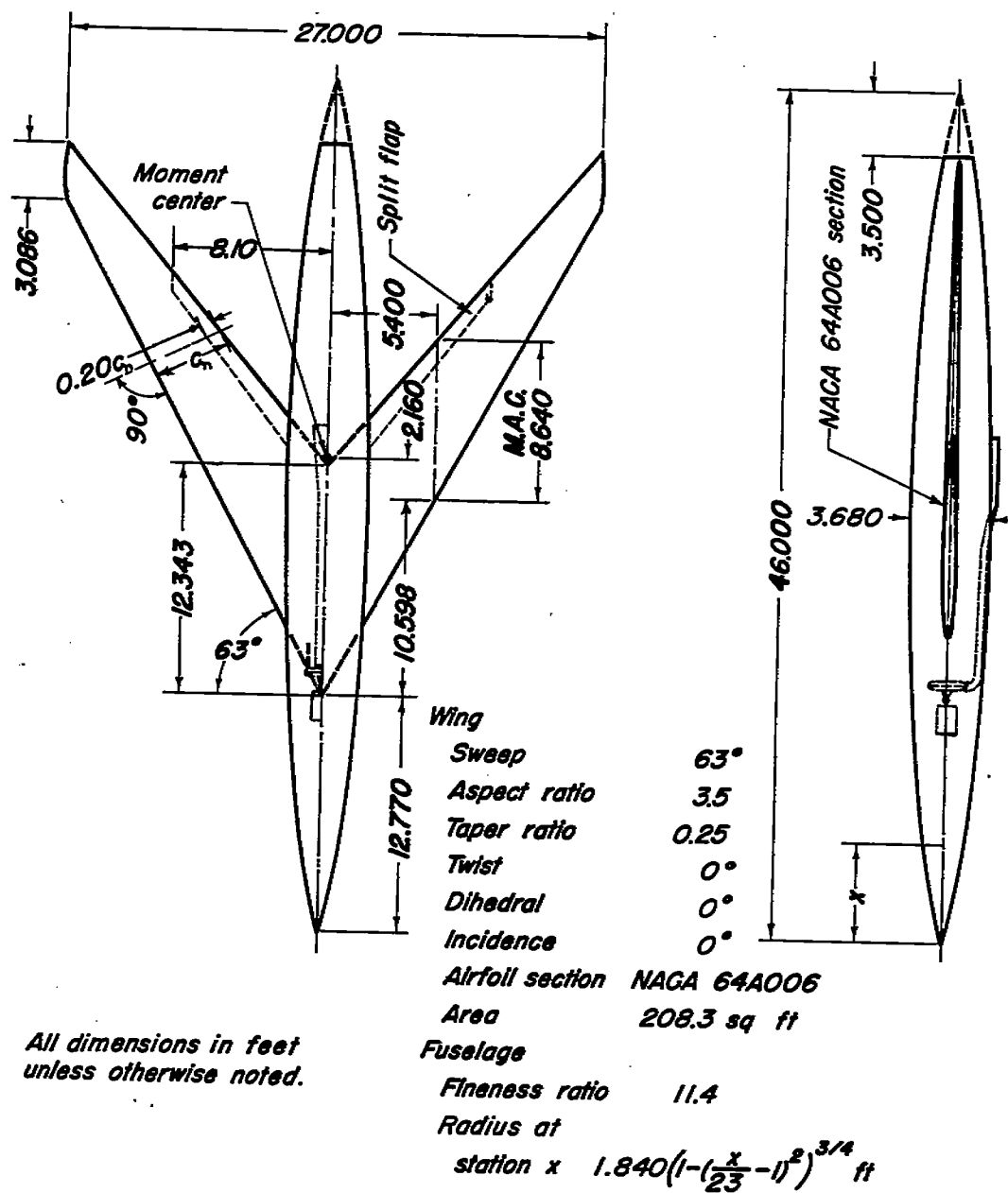
Figure 1.—Geometric characteristics of the 63° swept-back wing with fuselage.

Figure 2.— The 63° swept-back wing with fuselage mounted in the Ames 40- by 80-foot wind tunnel.

Metal mesh sheet

Metal mesh sheet covered
with nonporous tape

d

.20 c

.05 c

c

Streamwise section

€. Fuselage

.30 b/2

.45 b/2

.60 b/2

.75 b/2

.90 b/2

b/2

Straight line

d_1

d_2

d_3

d_4

d_5

Straight line

Model Configuration	Percent Local Streamwise Chord				
	d_1	d_2	d_3	d_4	d_5
A	1.4	2.6	3.8	4.8	6.2
B	1.0	2.0	3.1	4.0	5.2
C	0.6	1.4	2.3	3.2	4.2
D	0.3	0.7	1.2	2.1	4.2

NACA
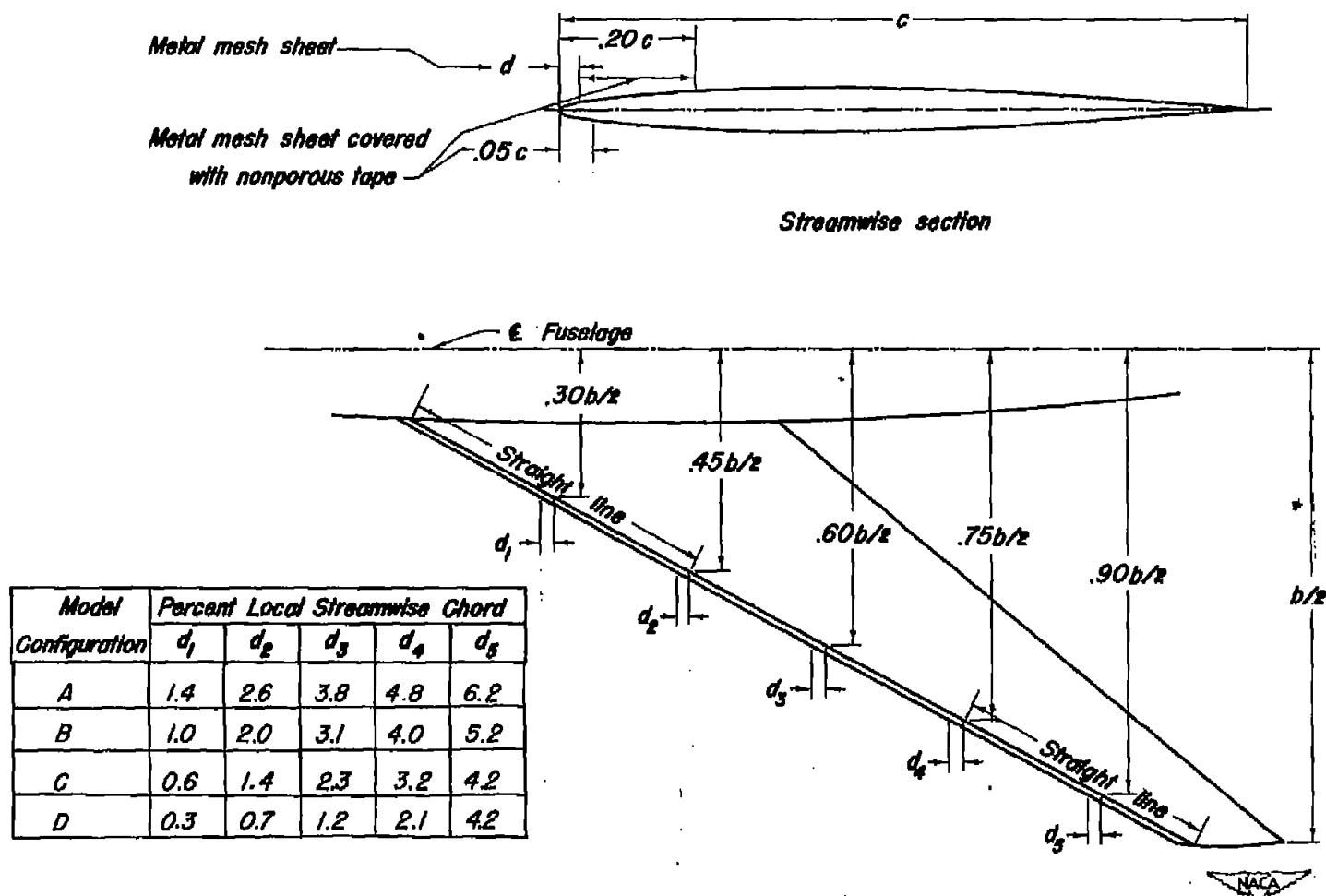
Figure 3.— Schematic drawing of the extent of porous area used in various configurations.

24

NACA RM A51J24
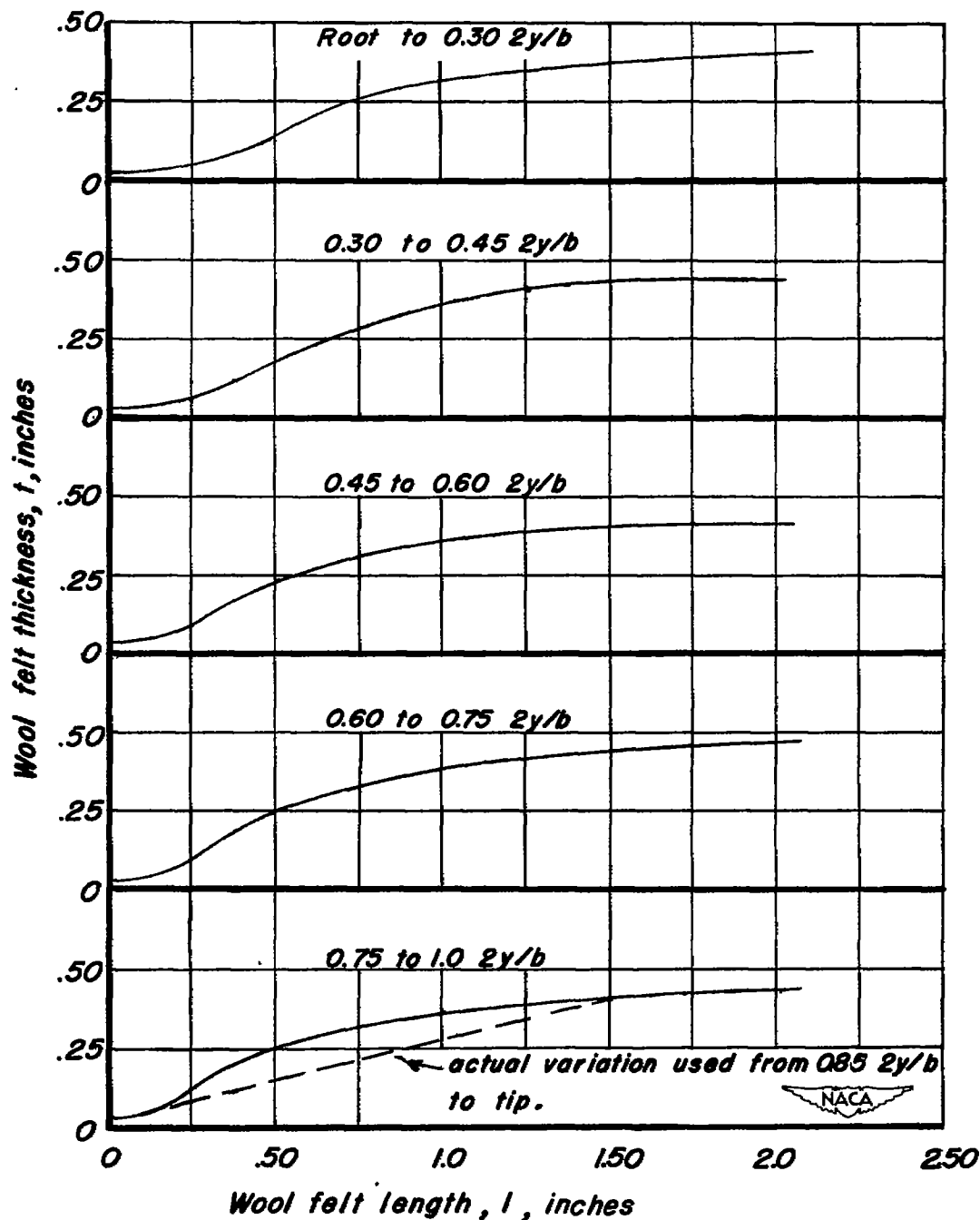
Figure 4.—Thickness variation of the wool felt for the five
spanwise groups of felts used for the porous leading
edge of the 63° swept-back wing.
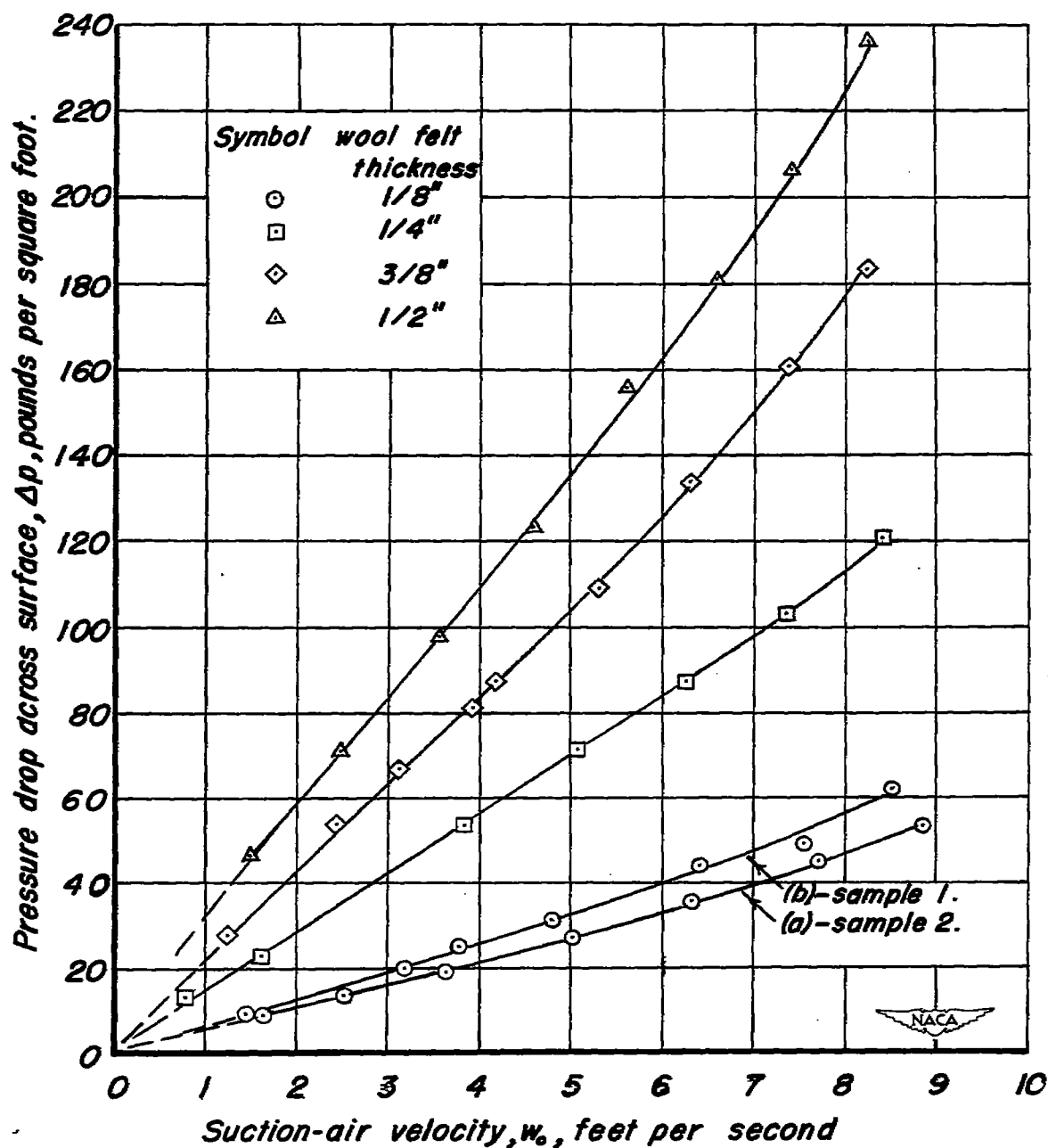
Figure 5 .— Calibration of suction-air velocities for the porous mesh sheet backed with various thickness of wool felt material.
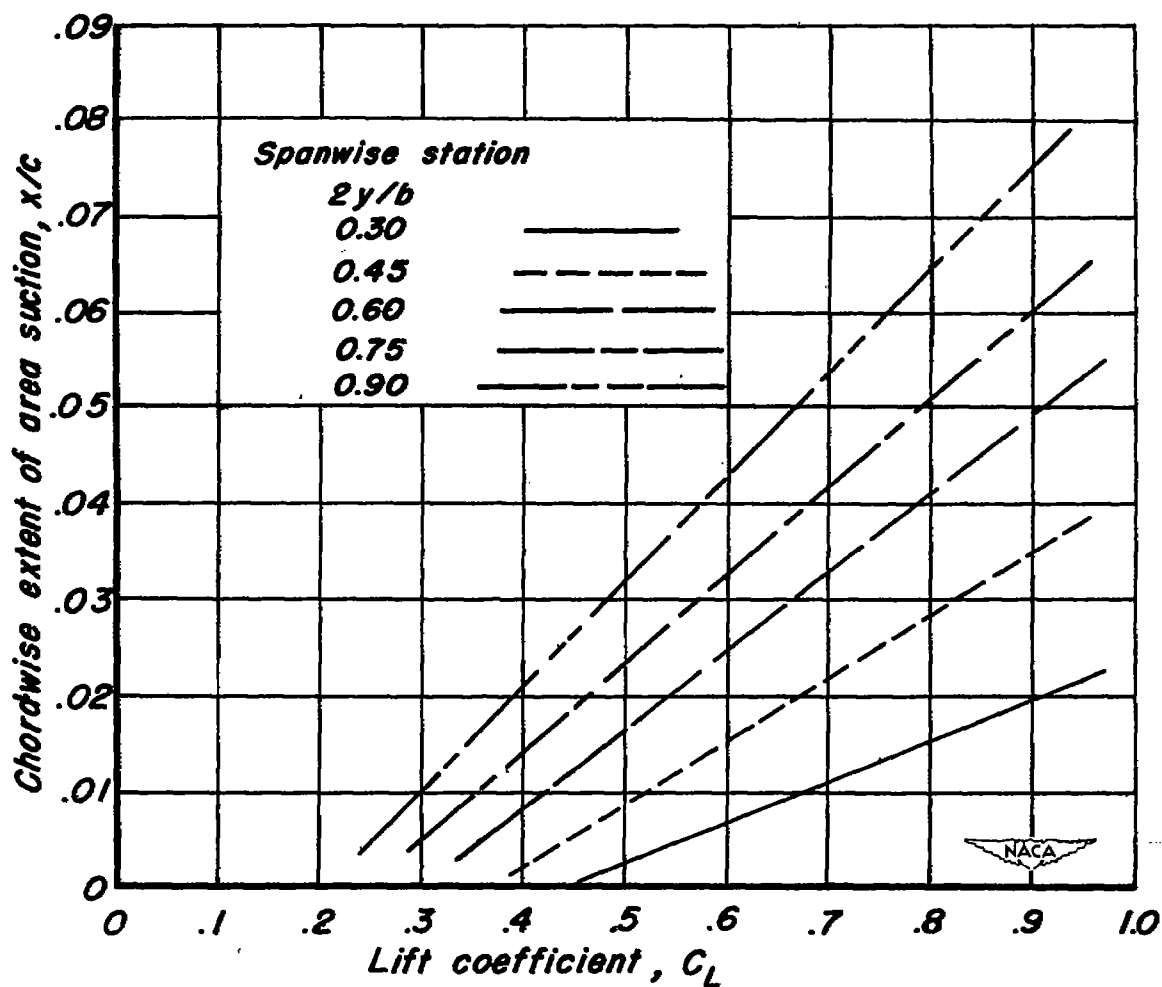
Figure 6 .—Estimations of the chordwise extent of area suction required to maintain unseparated flow on the 63° swept-back wing.
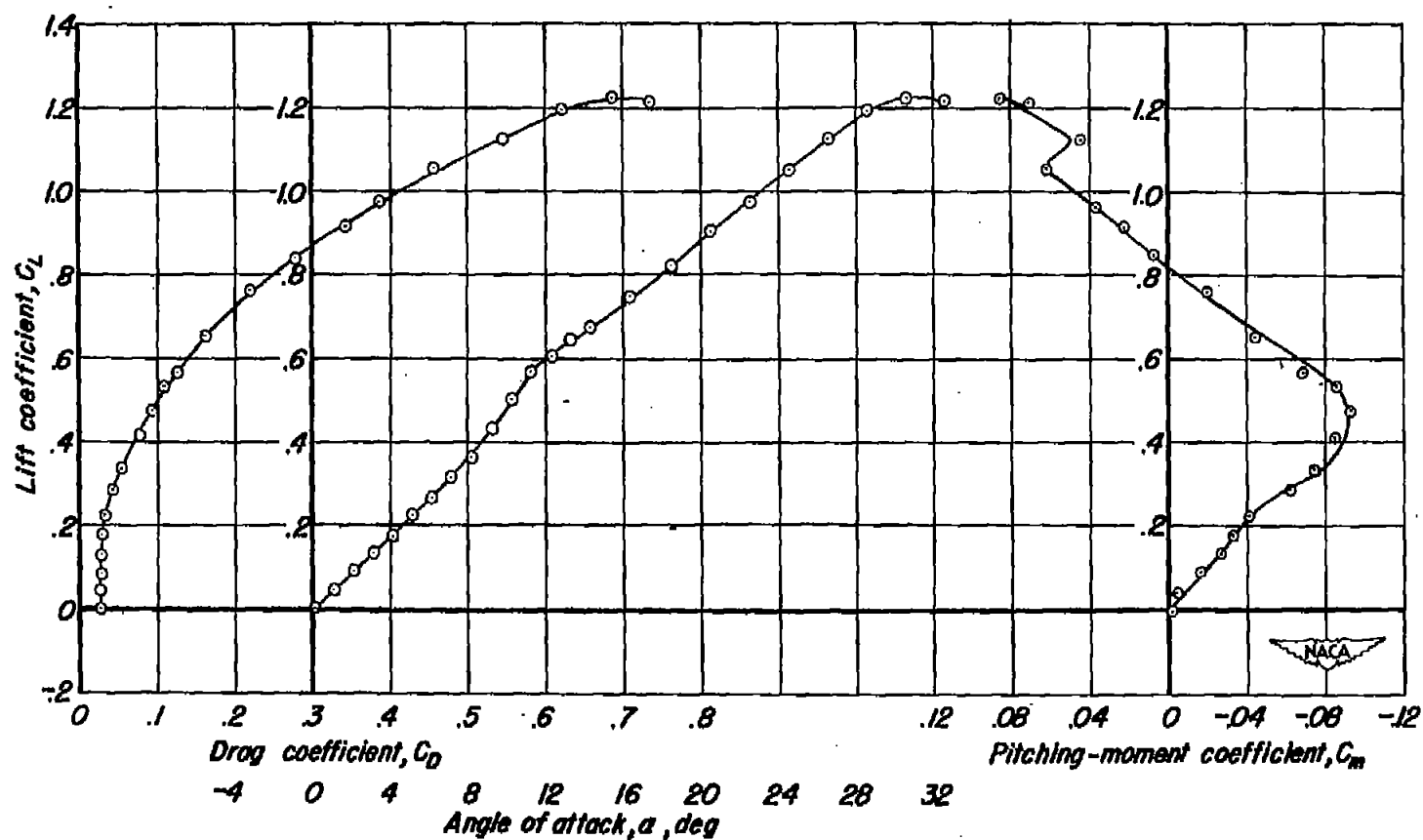
Figure 7.—The aerodynamic characteristics of the basic 63° swept-back wing.
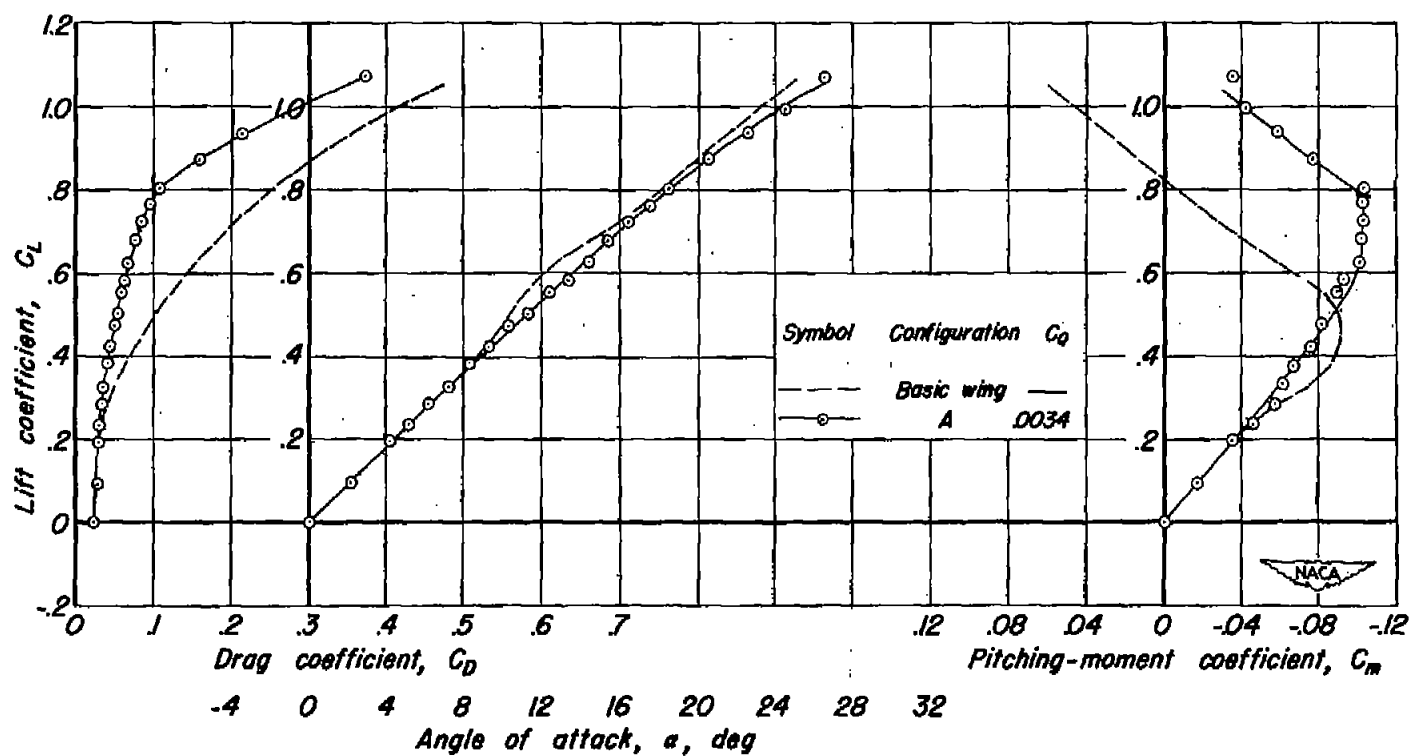
Figure 8 .—The effect of applying area suction with the suction—air velocities approximately equal at all chordwise points on the aerodynamic characteristics of the 63° swept-back wing. R = 5.2 x 10⁶.

Unflagged symbols indicate
upper surface.

Flagged symbols indicate
lower surface.

(a) $a=0.0°$
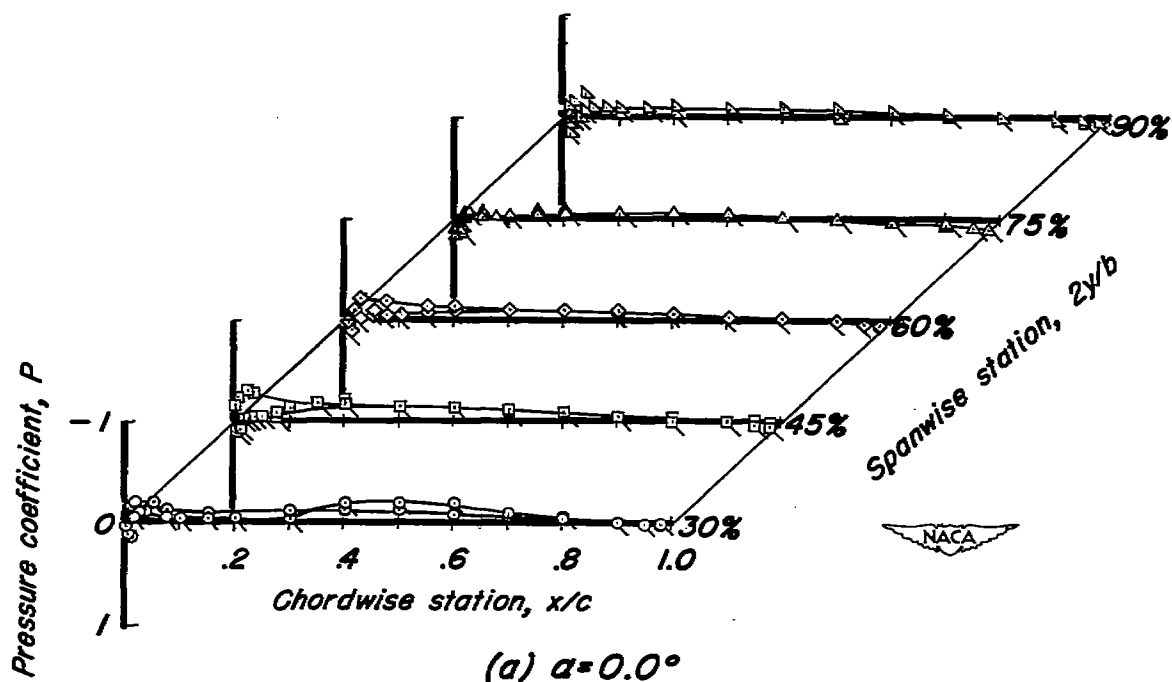
Figure 9 .—Chordwise pressure distribution of the
63° swept-back wing with area suction. Con-
figuration A. $C_Q = 0.0034$.

Unflagged symbols indicate
upper surface.

Flagged symbols indicate
lower surface.

(b) a=8.2°

Figure 9 .— Continued.

Symbol	x/c	P
△	0	−14.6
△	.0025	−14.9
◣	0	−12.3
◣	.0025	−13.4
◣	.0050	−11.4

Unflagged symbols indicate upper surface.

Flagged symbols indicate lower surface.

Pressure coefficient, P

Spanwise station, 2y/b

90%

75%

60%

45%

30%

Chordwise station, x/c

.4   .6   .8   1.0

NACA

(c) α=12.3°

Figure 9.—Continued.

Symbol	x/c	P
◇	0	−14.6
△	0	−16.3
△	.0025	−14.6
◺	0	−14.7
◺	.0025	−15.6
◺	.0050	−13.3

Unflagged symbols indicate upper surface.

Flagged symbols indicate lower surface.

Pressure coefficient, P

Spanwise station, 2y/b

Chordwise station, x/c

(d) α=14.3°

Figure 9 .—Continued.

Symbol	x/c	P
⊡	0	−16.7
◇	0	−18.7
△	0	−21.0
◮	.0025	−19.0
◭	.0050	−14.5
◪	0	−18.5
◪	.0025	−19.2
◪	.0050	−16.2
◪	.0025	−13.1

Unflagged symbols indicate upper surface.

Flagged symbols indicate lower surface.

(e) a=16.4°

Figure 9 .— Continued.

Symbol	x/c	P
▫	0	−18.2
▫	.0025	−14.6
◇	0	−20.9
△	0	−22.8
⟟	.0025	−19.8
△	.0050	−15.9
⟟	.0025	−14.2
⟟	0	−19.7
⟟	.0025	−20.2
⟟	.0050	−17.0

Unflagged symbols indicate upper surface.

Flagged symbols indicate lower surface.

(f) α=17.4°

Figure 9 −Continued.

Symbol	x/c	P
⊡	0	−22.0
⊟	.0025	−17.6
◇	0	−23.3
◇	.0025	−14.6
◈	.0025	−14.5
△	0	−23.3
△	.0025	−15.0
△	.0050	−12.6
◮	0	−20.0
◮	.0025	−20.0
◮	.0050	−16.6
◮	.0025	−14.6

Unflagged symbols indicate upper surface.

Flagged symbols indicate lower surface.

Pressure coefficient, P

Chordwise station, x/c

Spanwise station, 2y/b

90%
75%
60%
45%
30%

(g) α=18.4°

Figure 9 .— Continued.

Symbol	x/c	P
⊙	0	−17.5
▫	0	−26.6
▫	.0025	−19.0
▫	.0050	−16.7
◧	.0025	−15.1
◇	0	−23.5
◇	.0025	−16.8
◆	.0050	−13.8
◈	.0025	−15.4
△	0	−21.1
▲	.0025	−16.0
▲	.0050	−13.2
◺	0	−16.8
◺	.0025	−16.4
◺	.0050	−13.1
◹	.0025	−12.4

Unflagged symbols indicate
upper surface.

Flagged symbols indicate
lower surface.

(h) a=20.4°

Figure 9 .— Continued.

Symbol	x/c	P
⊙	0	−23.8
⊙	.0025	−22.5
⊾	.0025	−16.7
▫	0	−26.3
▫	.0025	−20.8
▫	.0025	−16.0
▫	.0050	−14.6
△	0	−17.4
△	.0025	−13.7
▷	0	−16.2
▷	.0025	−15.2
▷	.0050	−12.5
▷	.0025	−12.4

Unflagged symbols indicate upper surface.

Flagged symbols indicate lower surface.

(i) a=24.5°

Figure 9.—Concluded.

Figure 10.-Variation of pressure coefficient with angle of attack at four chordwise locations at 90-percent span on the 63° swept-back wing with the application of area suction. Configuration A. $C_Q = 0.0034$.
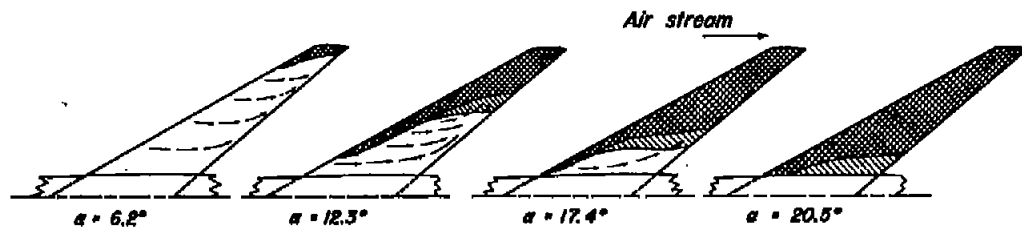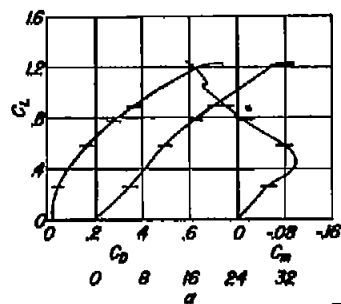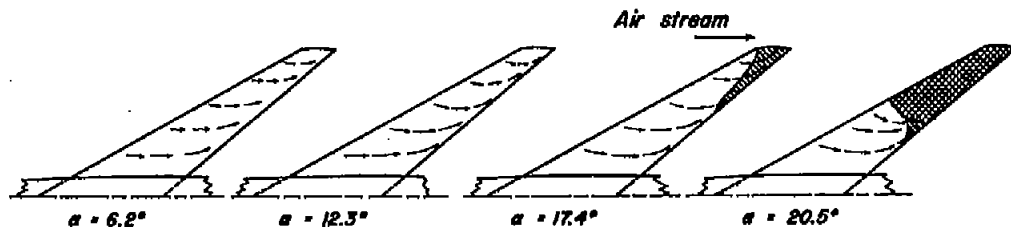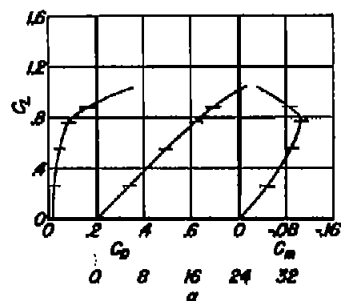
Figure 11. — Flow studies with and without area suction on the 63° swept-back wing. Configuration A.
R = 5.2 x 10⁶.
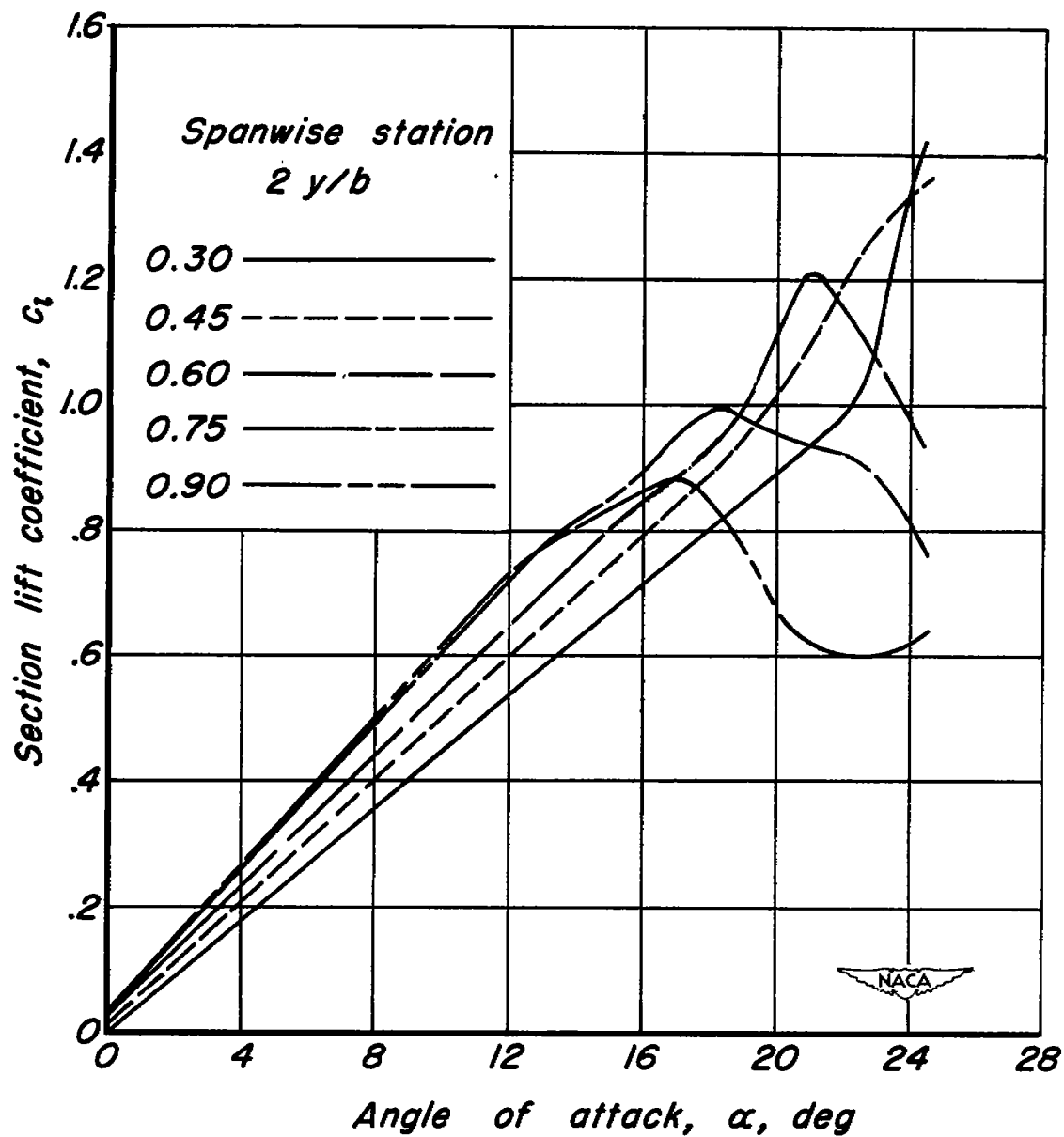
Figure 12.— Section lift curves of the 63° swept-wing with area suction applied. Configuration A. $C_Q = 0.0034$.
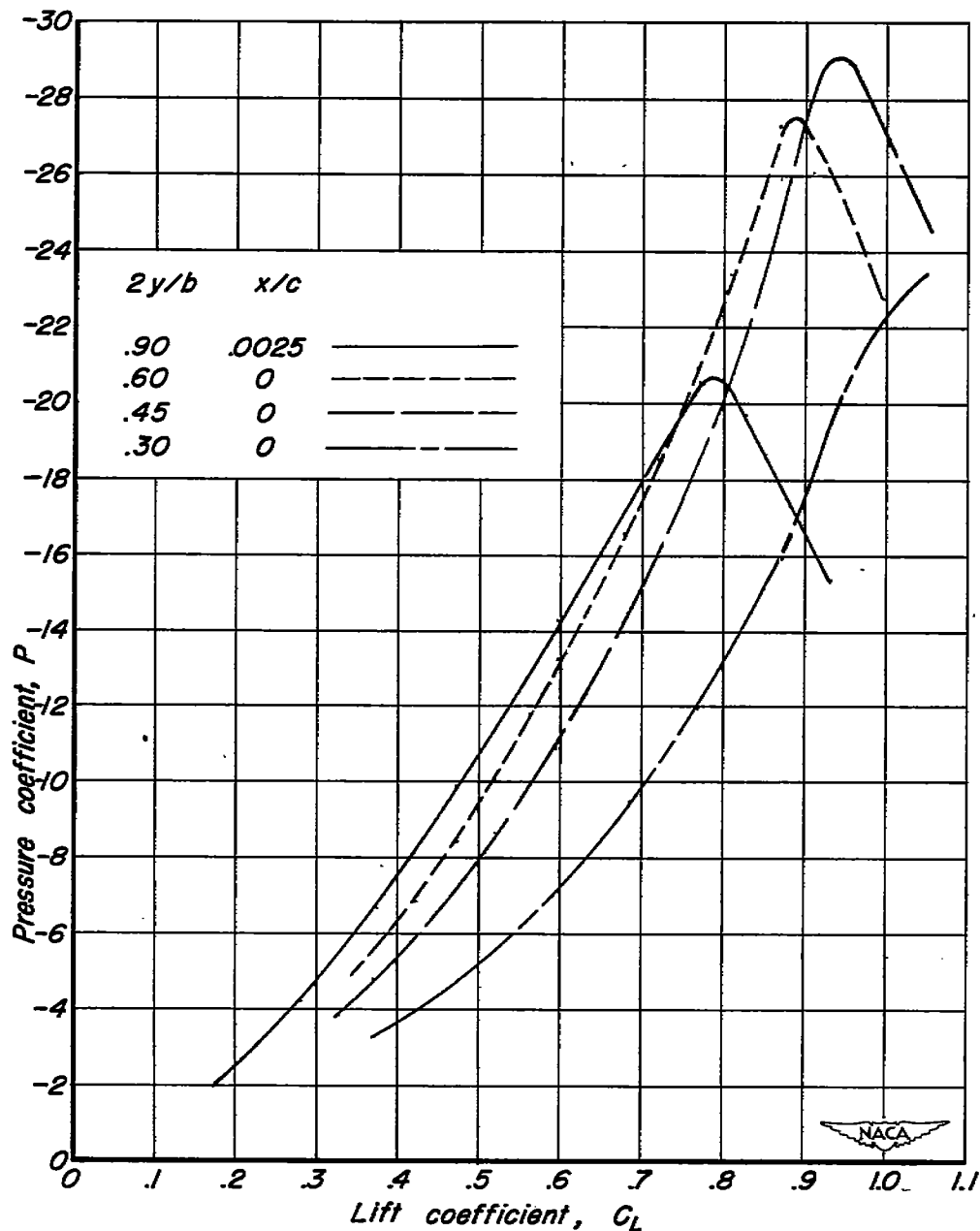
Figure 13 .-Variation of pressure coefficient with lift coef-
ficient near the leading edge of the 63° swept-back
wing at four spanwise sections with the application of
area suction. Configuration A. C_Q = 0.0034 .
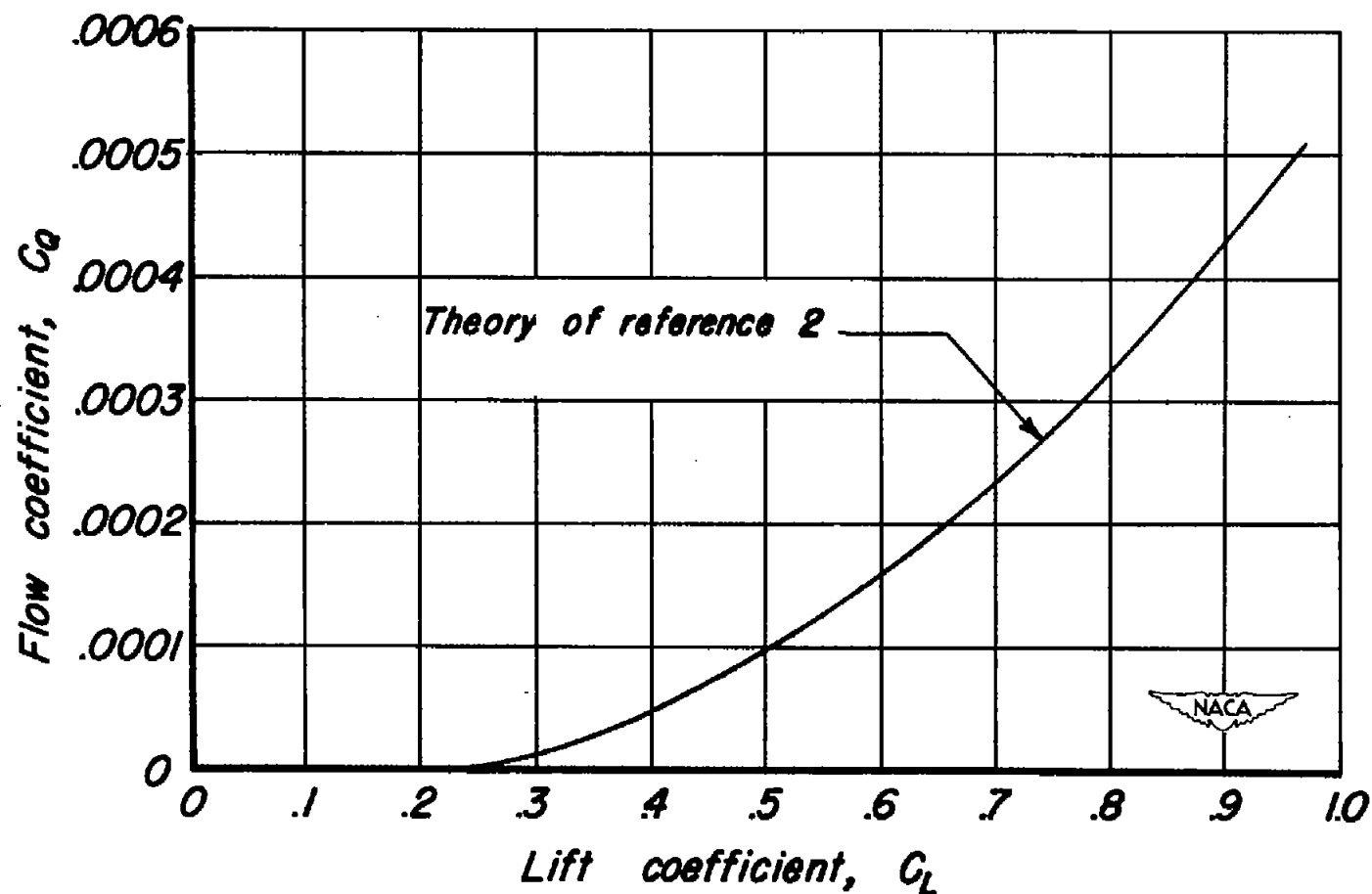
Figure 14.— Theoretical flow coefficients as a function of lift coefficient for the 63° swept-back wing.
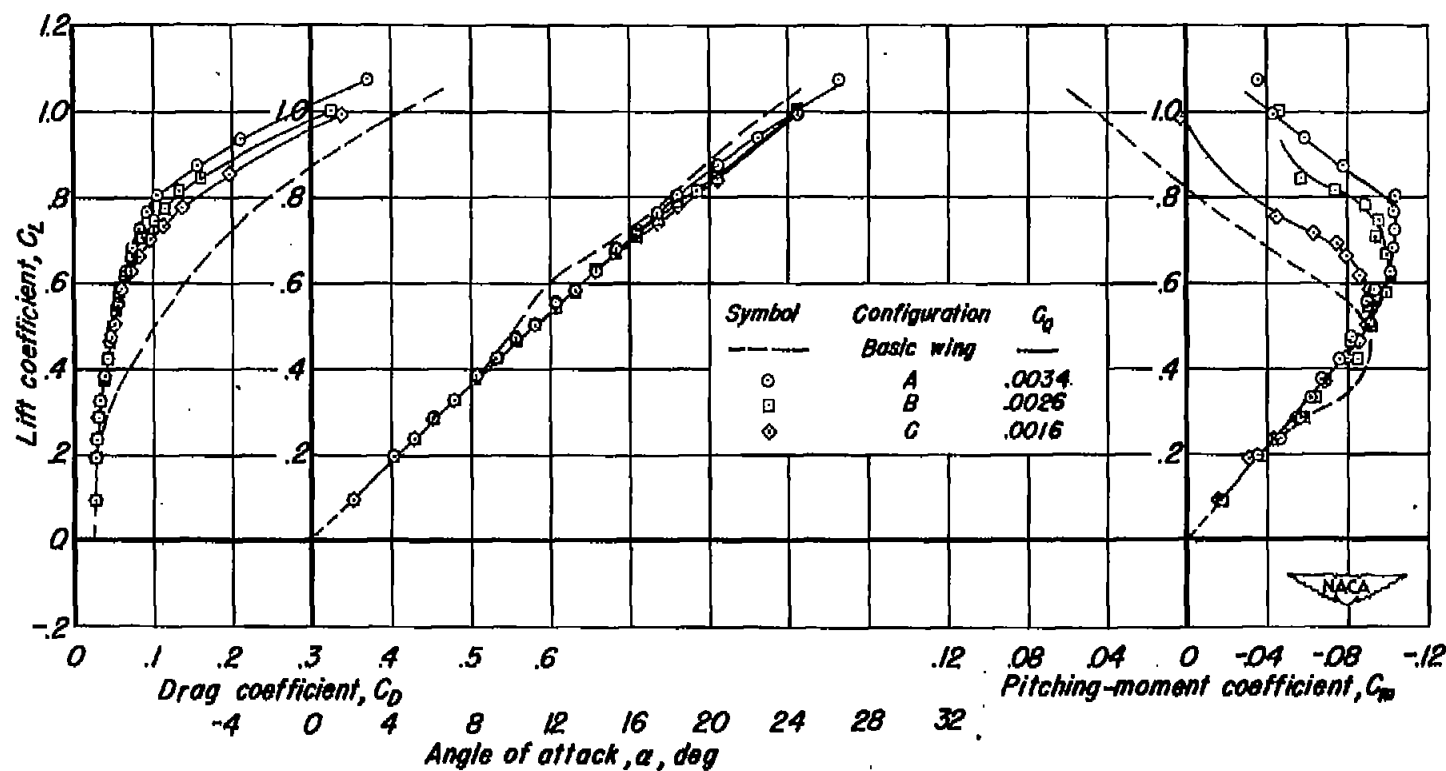
Figure 15.— The effect of applying area suction with the suction-air velocities approximately equal at all chordwise points on the aerodynamic characteristics of several configurations of the 63° swept-back wing. R=5.2×10⁶.
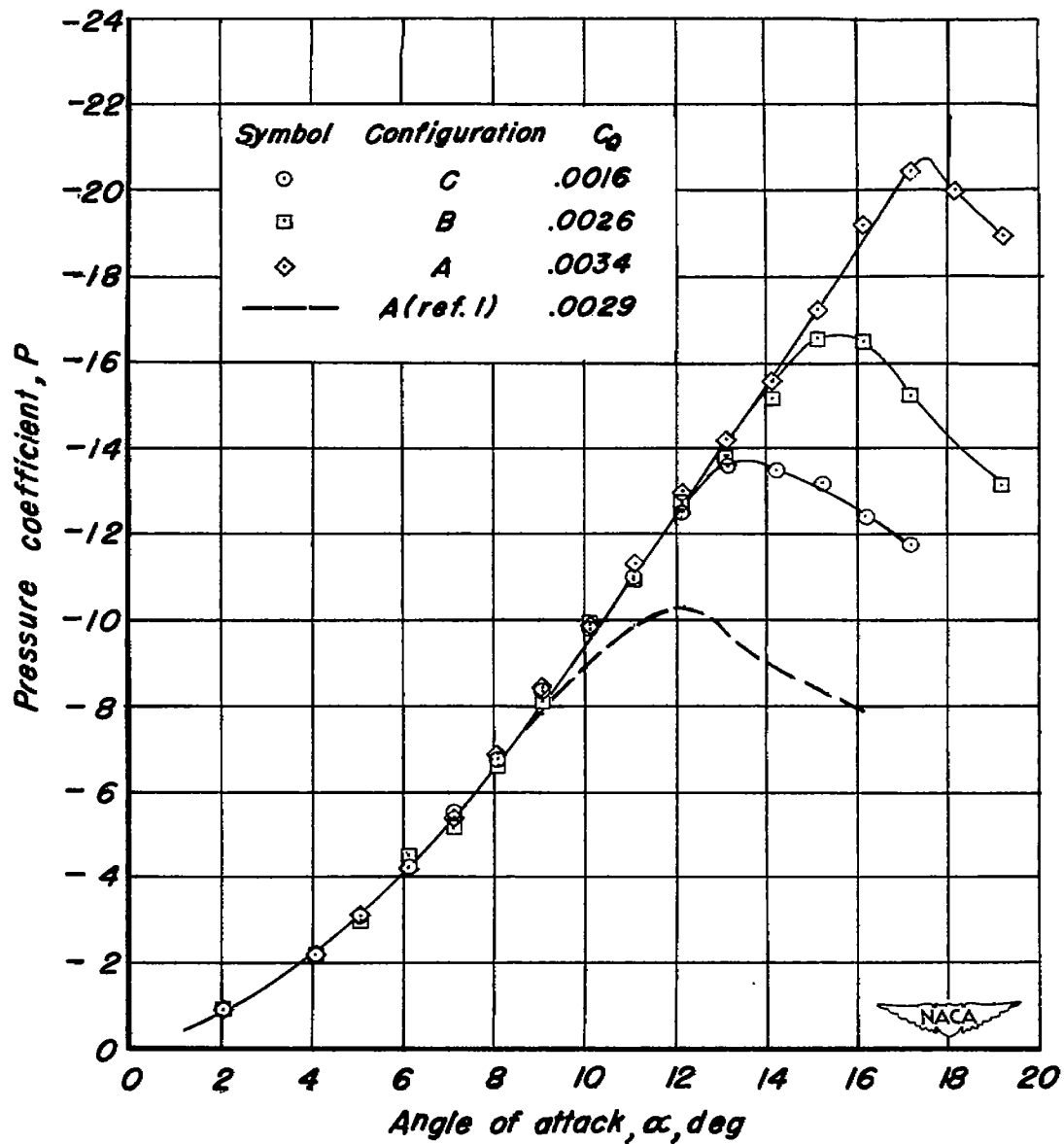
Figure 16 .— Variation of pressure coefficient at 0.25-per-
cent chord and 90-percent span station with
angle of attack for four configurations of area
suction.
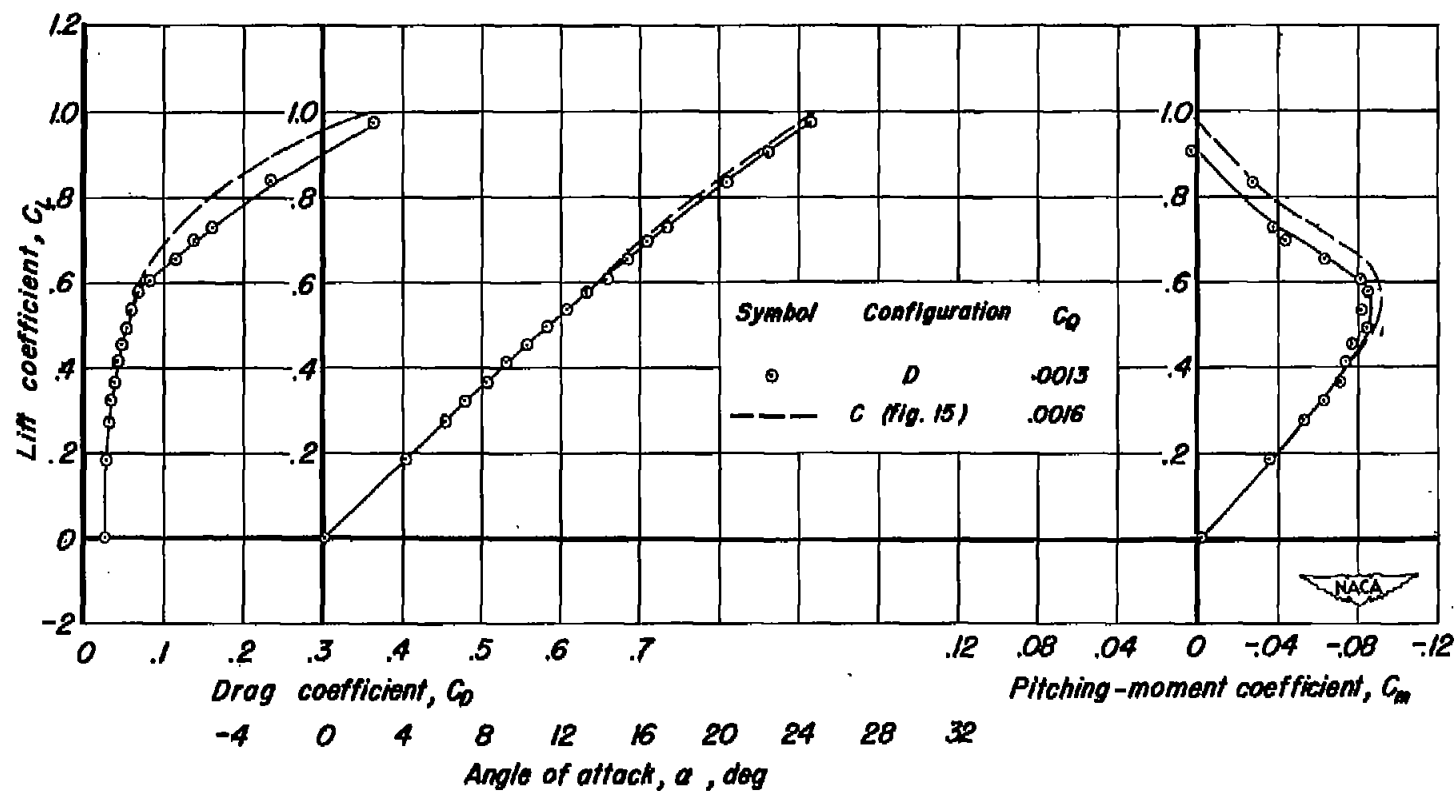
Figure 17.—The effect of reducing the chordwise extent of area suction at the inboard sections of the wing on the aerodynamic characteristics of the 63° swept-back wing. Configuration D. R=5.2x10⁶.
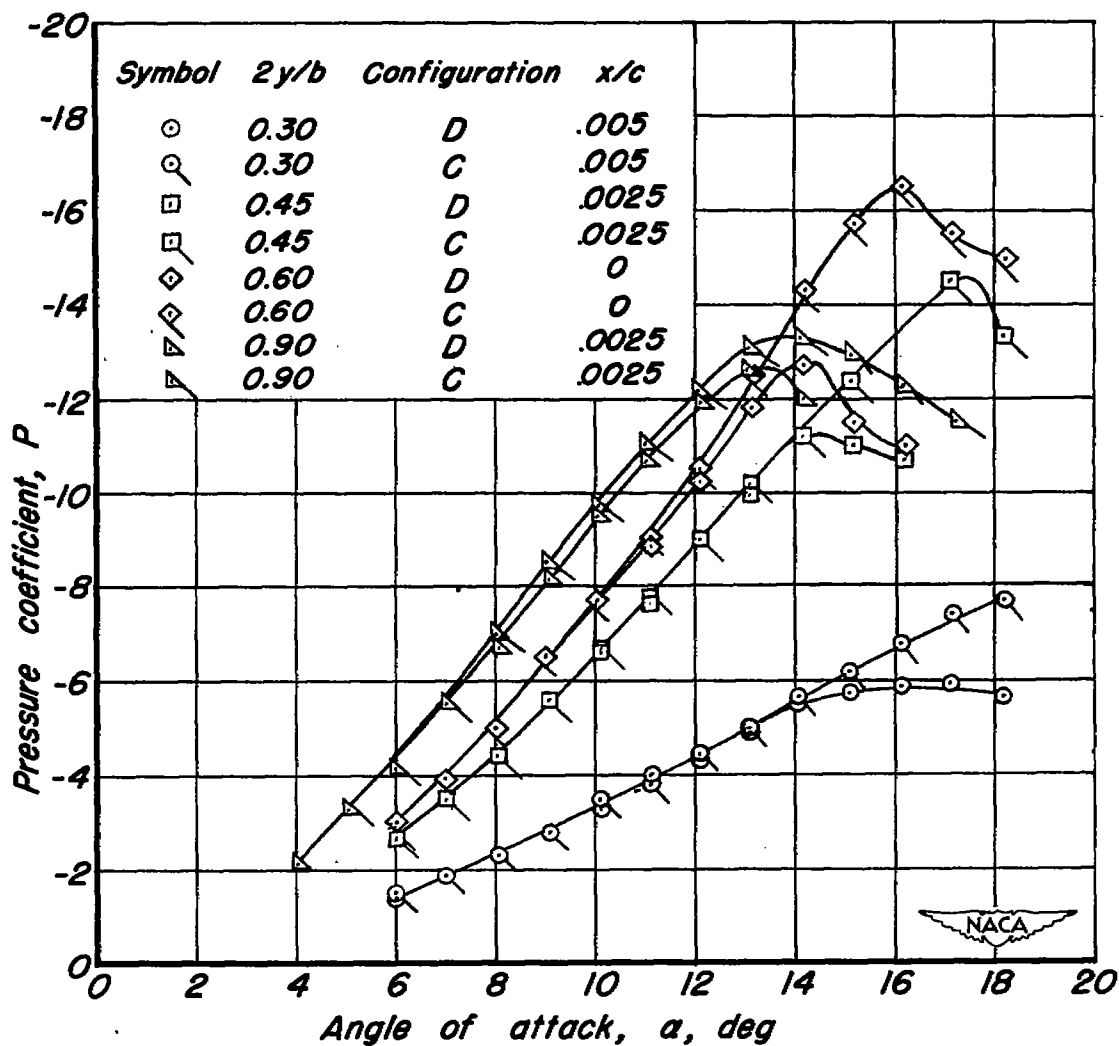
Figure 18.— Variation of pressure coefficient near leading edge at several spanwise sections for configurations C and D.
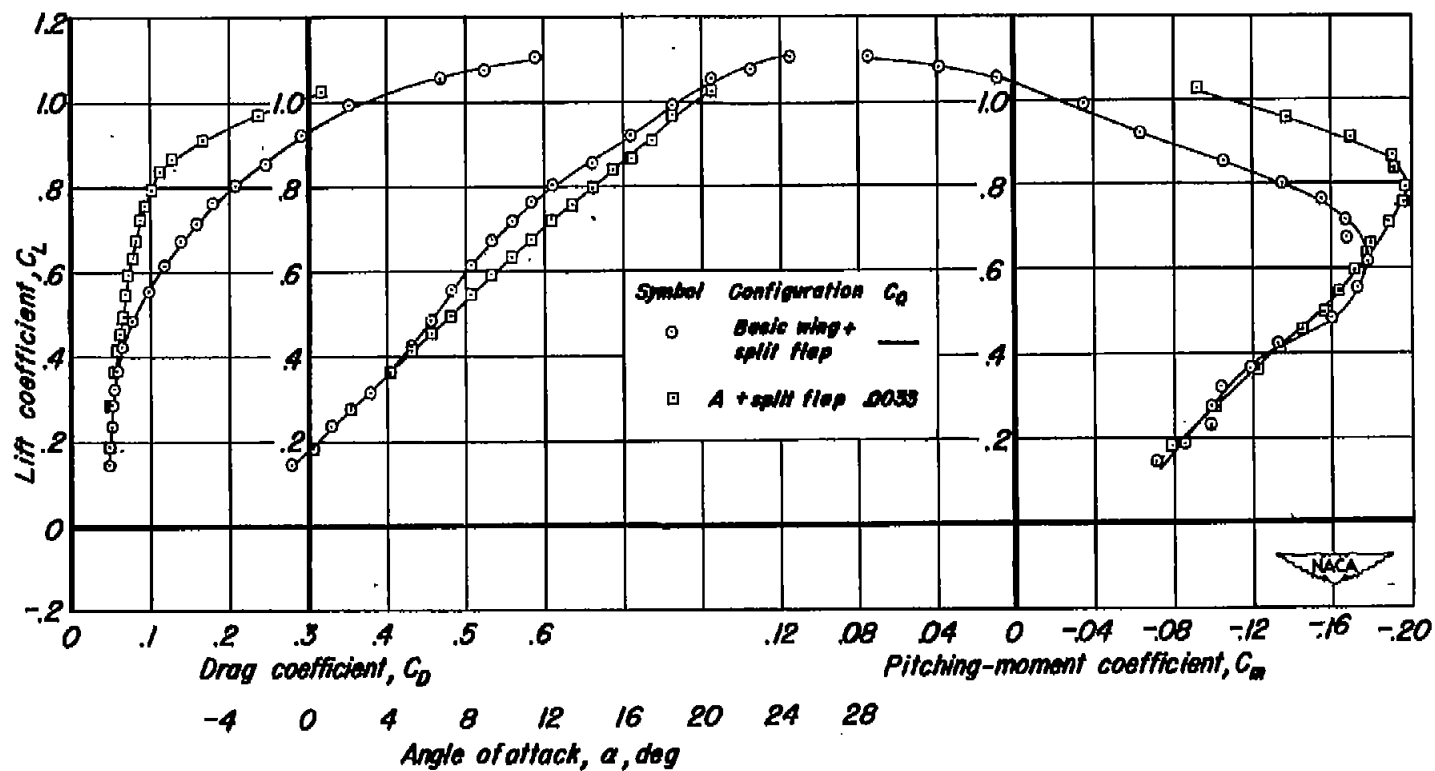
Figure 19.—The effect of area suction application on the aerodynamic characteristics of the 63° swept-back wing with a trailing-edge split flap deflected down 45°. R=5.2×10⁶
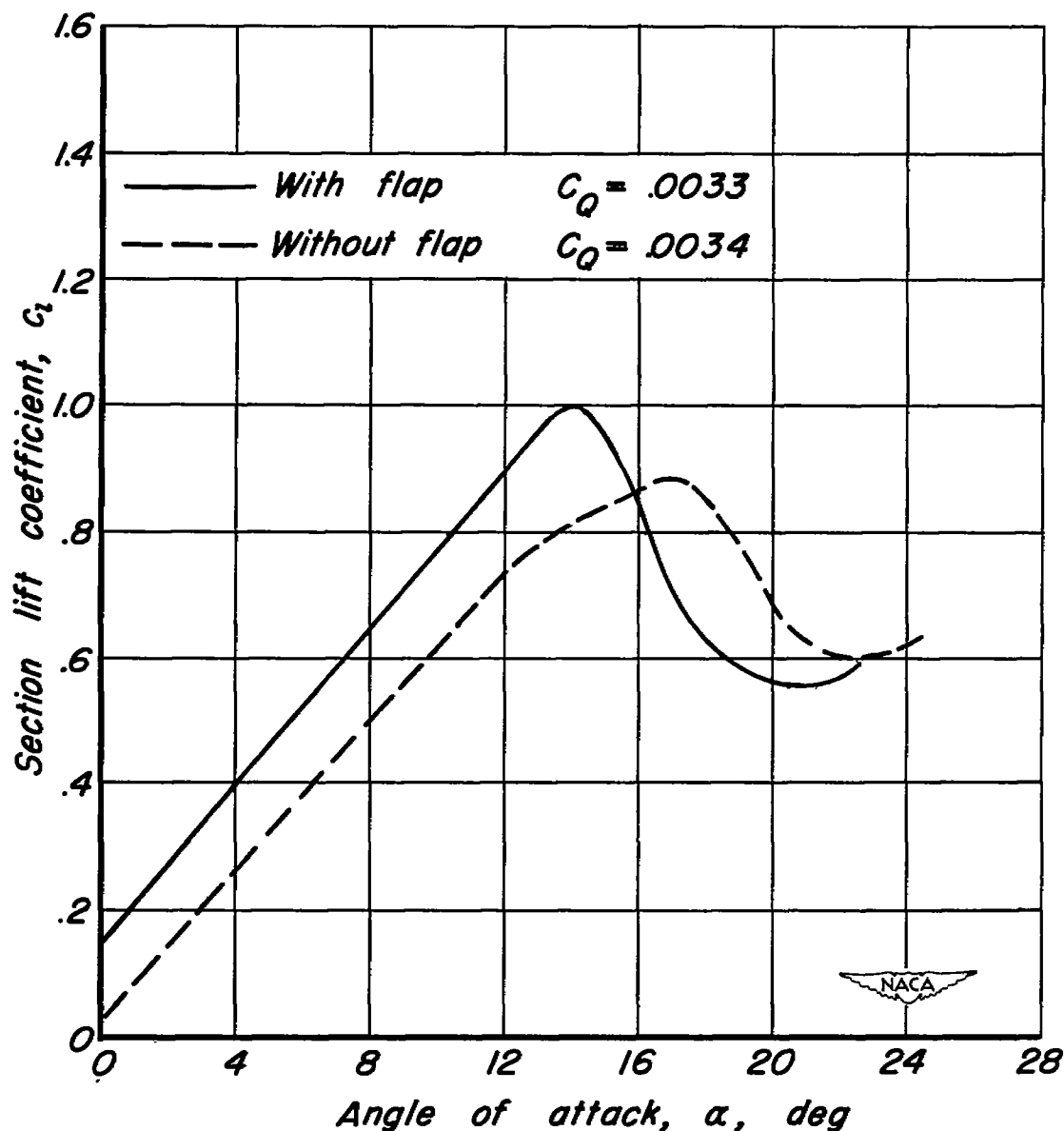
Figure 20.— Section lift coefficient curves at the 90-percent spanwise section with and without a trailing-edge split flap to 60-percent span on the 63° swept-back wing. Area suction applied.
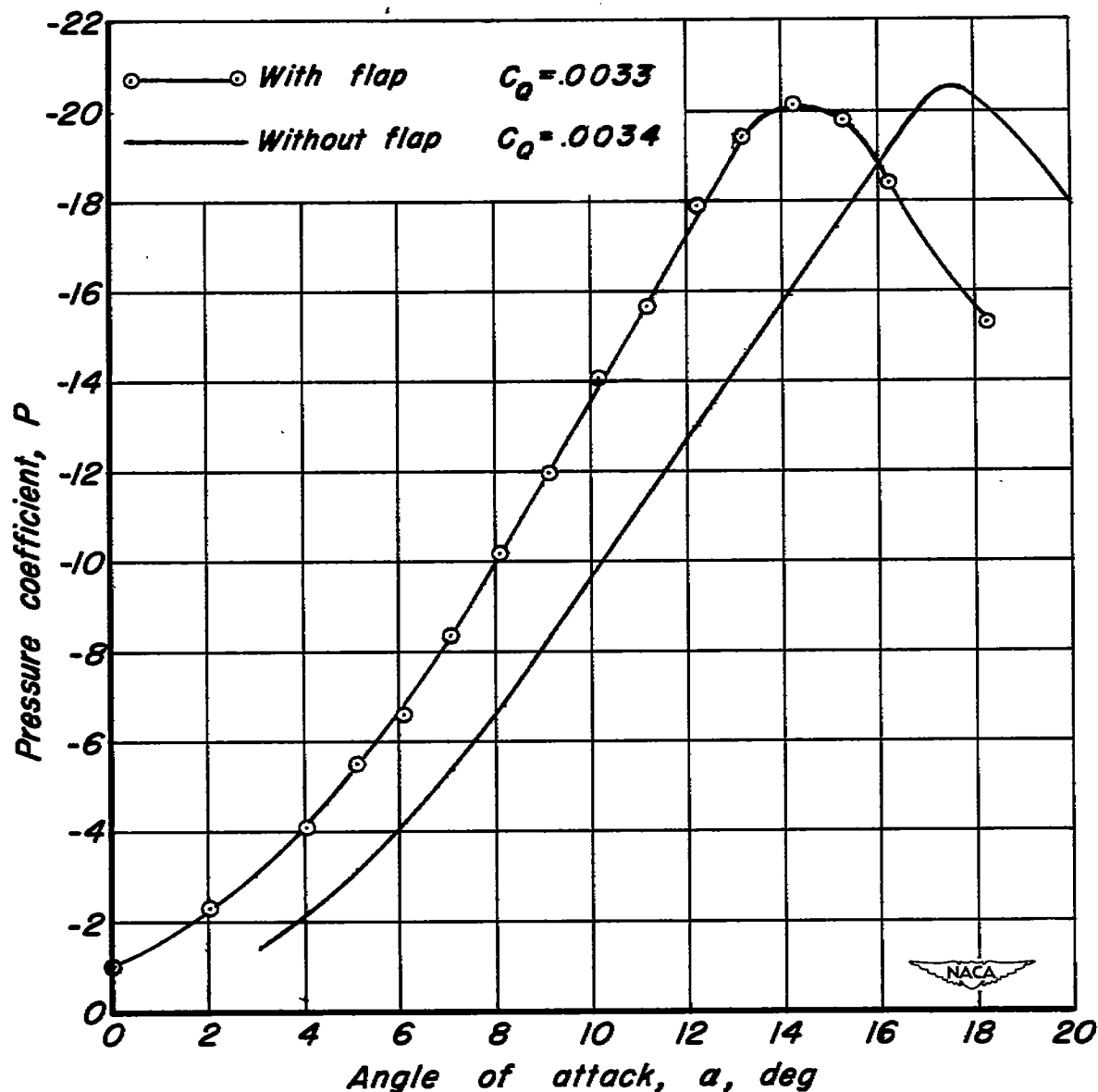
Figure 21.- Variation of pressure coefficient with angle of attack at 0.25 percent chord at 90-percent span for the 63° swept-back wing with and without a split flap and with area suction.
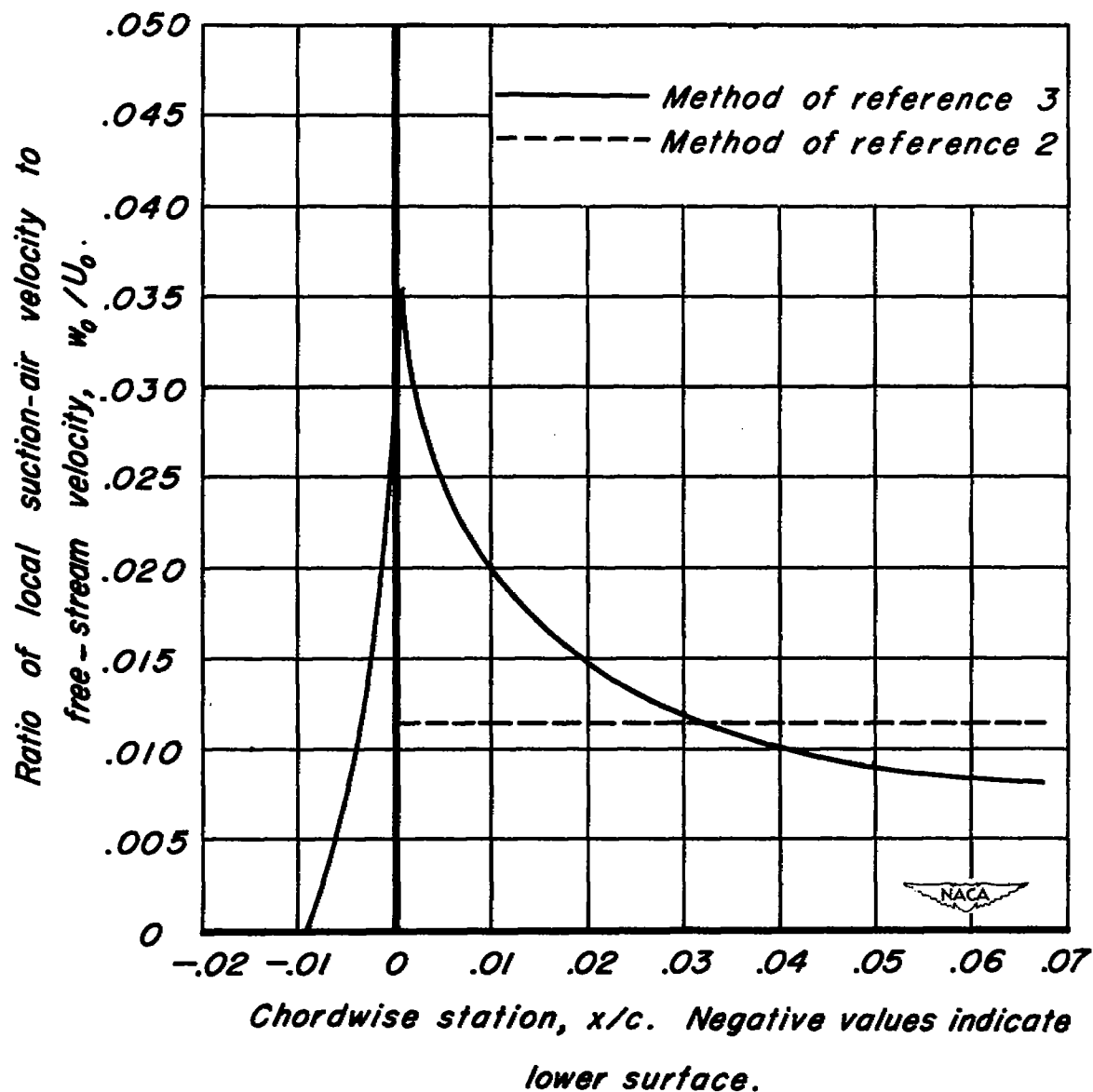
Figure 22.—Theoretical chordwise distribution of suction-air velocity for the 90-percent span station of the 63° swept-back wing at a lift coefficient of 0.77.
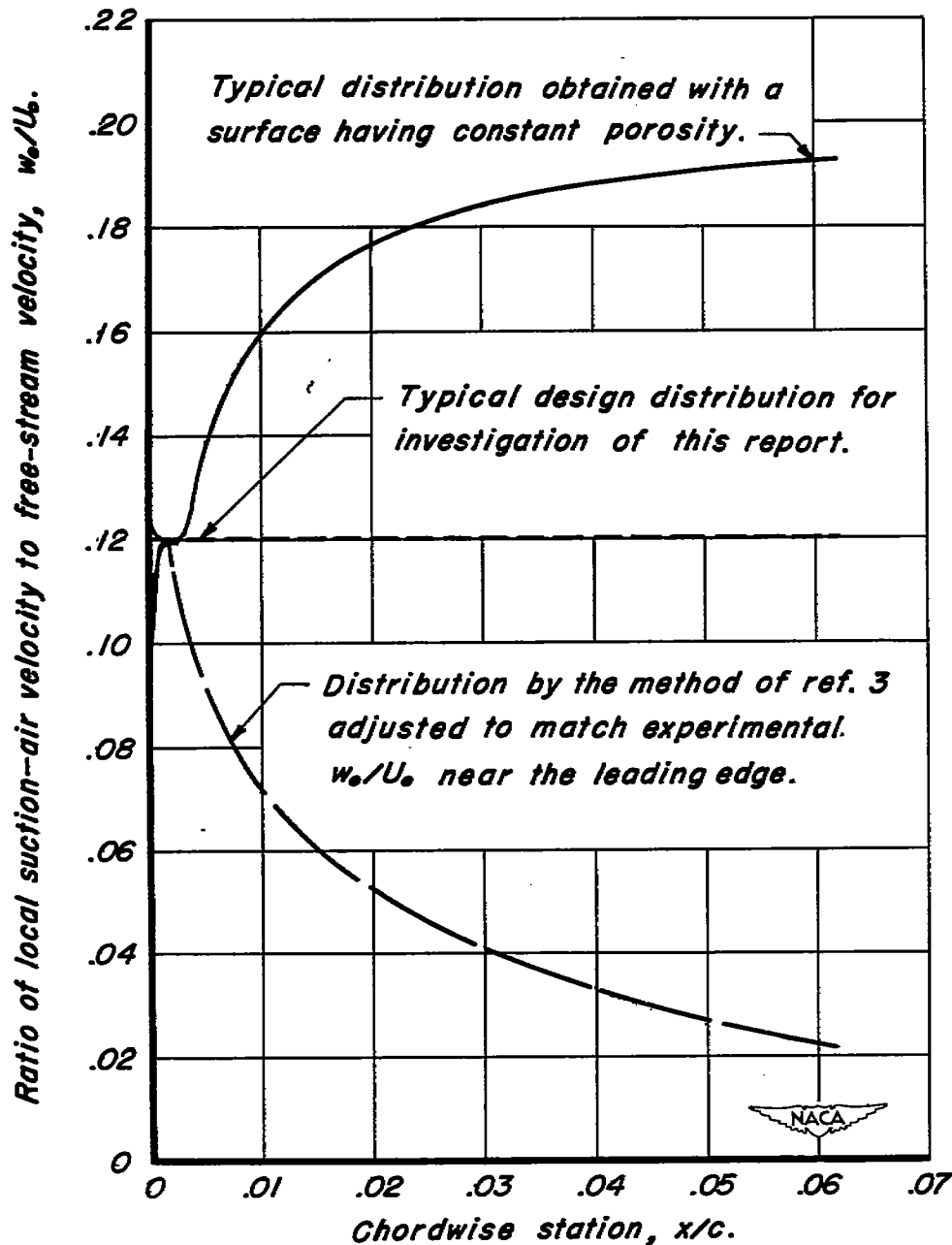
Figure 23.— Comparison of three chordwise distributions of suction-air velocity for equal required velocities near the leading edge.